ASIFA KASHIF

MODELING AND COMPENSATION OF TRANSCEIVER NON-RECIPROCITY IN TDD MULTI-ANTENNA BASE-STATION

Master of Science Thesis

ABSTRACT

ASIFA KASHIF: Modeling and Compensation of Transceiver Non-Reciprocity in TDD Multi-Antenna Base-Station
Tampere University of Technology
Master of Science Thesis, 48 pages, 0 Appendix page
March 2015
Master's Degree Programme in Electrical Engineering
Major: Wireless Communication Circuits and Systems
Examiners: Professor Mikko Valkama, Postdoctoral Researcher Zou Yaning

Keywords: transceiver non-reciprocity, MU MIMO-OFDM, channel reciprocity, estimation, compensation.

Due to the increasing demands for higher system capacity, higher data rates and better quality of service in wireless networks, advanced techniques that improve wireless link reliability and spectral efficiency are introduced. This includes different multi-antenna technologies, in particular multi-user (MU) MIMO-OFDM. In MU MIMO-OFDM systems, base-station with multiple antennas communicates simultaneously with multiple users over a given time-frequency resource. In downlink transmission, base-station transmits multiple data streams through its antennas towards the user devices. In uplink transmission, the user equipment send in parallel multiple data streams towards the base-station. In general, channel non-reciprocity is a very important factor in cellular communications, in particular in precoded MU MIMO-OFDM systems adopting time division duplexing (TDD). Based on the channel reciprocity principle, the channel state information at base-station for the downlink transmission can be determined through estimating the uplink channels. In practice, however, there are always unavoidable frequency mismatch characteristics between transmitter and receiver. Frequency response mismatch can thus change the reciprocal nature of downlink and uplink channels. The impact of transceiver non-reciprocity at equipment on user side causes inter-stream interference which can be compensated using detection processing. The impact of transceiver non-reciprocity at base-station causes inter-user interference and degrades the system performance of MU MIMO-OFDM systems.

To ensure the system reliability and high performance in case of transceiver non-reciprocity, some non-reciprocity estimation and compensation methods are required. The previous work has proposed the estimation-compensation framework that gives a flexible solution to restore the channel reciprocity. But there is a need to validate the findings and performance of the proposed estimation-compensation framework. The modeling of transceiver frequency response mismatch characteristics using actual measurement data has been carried out in this thesis research work. The actual measurement data comprises of one base-station with two antennas and two user equipment devices with single antenna. The estimated uplink and downlink channels from measurement data are used to compute the non-reciprocity matrix at base-station and at

the equipment on user side after mathematical calculations. The normalized parameters for transceiver non-reciprocity matrices are extracted subcarrier-wise. The frequency-domain normalized non-reciprocity parameters are modeled as a FIR filter in the time-domain and the most energy concentrates then on few time-domain taps. The extracted parameters are mildly frequency-selective. The impact of extracted transceiver non-reciprocity is then analyzed by implementing a simulator of TDD precoded MU MIMO-OFDM system.

In general, the frequency-selectivity implies that the reciprocity estimation and compensation is needed subcarrier-wise. The pilot-based estimation of non-reciprocity parameters at base-station is carried out in order to enhance the system performance. To estimate channel non-reciprocity parameters, a link between base-station and one of user equipment devices is assumed. The right choice of selecting the user is also important for noise reduction in estimation. For estimation, the DL transmission channel is modeled as a Rayleigh fading multipath channel with a given 7-tap channel power delay profile. The downlink data including sparsely located pilots at selected subcarriers is transmitted to the user through downlink channel without precoding. The downlink channel is then estimated at the user equipment side. This provides estimates only at the pilot subcarriers. Therefore, linear interpolation is used to obtain channel response estimates at the actual data subcarriers. The uplink pilot data is transmitted to base-station from user equipment through uplink channel. The uplink channel is obtained by estimated downlink channel in case of non-reciprocity parameters. Then, estimate of non-reciprocity at base-station is computed by using inverse processing and an interpolator. The estimated parameters are used as a compensator filter in order to compensate the channel non-reciprocity in the system.

The simulated results show that the performance deviates from the ideal linear precoded MU MIMO-OFDM system because of non-reciprocity in case of both error control coded and uncoded channels. The compensated results in terms of coded and uncoded channel schemes have been evaluated which are closer to ideal linear precoded MU-MIMO OFDM system. These results show that the impact of non-reciprocity on system performance is less severe when a coded channel is deployed as compared to uncoded channel. The modeling of transceiver frequency response mismatch characteristics using actual measurement data proves that the proposed non-reciprocity model in the previous research work is close to reality.

PREFACE

This Master of Science thesis is written in the Department of Electronics and Communications, Tampere University of Technology, Finland. The work has been carried out as a Research Assistant and is presented in this thesis.

I am thankful to my supervisors, Professor Mikko Valkama and Postdoctoral Researcher Zou Yaning, for their continuous support, valuable guidance and timely feedback. I would also like to thank both of them for their welcoming attitude and professional advices on different stages during my research work. I would like to express my gratitude to Dr. Per Zetterberg from Qamcom Research and Technology for his cooperation regarding the provision of measurement data.

I am grateful to my parents and family for their love, patience and good wishes in connection with my thesis work. Last but not least, I would like to thank my husband, Kashif Javed, for his untiring assistance and caring attitude which has enabled me complete this work in accordance with set time schedule.

Tampere, 15.10.2015

Asifa Kashif

CONTENTS

LIST OF FIGURES

LIST OF TABLES

LIST OF SYMBOLS AND ABBREVIATIONS

MIMO	Multiple Input Multiple Output
MU-MIMO	Multi-User MIMO
SU-MIMO	Single-User MIMO
3G	Third Generations
LTE	Long Term Evolution
3GPP	Third Generation Partnership Project
WLAN	Wireless Local Area Network
OFDM	Orthogonal Frequency Division Multiplexing
ZF	Zero Forcing
BER	Bit Error Rate
SNR	Signal-to-Noise Ratio
FFT	Fast Fourier Transform
TDD	Time Division Duplexing
CSI	Channel State Information
BS	Base-Station
UE	User Equipment
MS	Mobile Station
Tx	Transmitter
Rx	Receiver
FR	Frequency Response
IUI	Inter-User Interference
LOS	Line-of-Sight
NLOS	Non line-of-sight
φ	Phase
σ_s^2	Signal Variance
σ_n^2	Noise Variance
σ	Standard Deviation
$\lvert\ \rvert$	Absolute
$(.)^{-1}$	Inverse
$(.)^{T}$	Transpose
$\mathbf{A}_b$	Non-Reciprocity Matrix at BS
$\mathbf{A}_u$	Non-Reciprocity Matrix at UE
$\mathbf{H}_{UL}$	Uplink Channel Matrix
$\mathbf{H}_{DL}$	Downlink Channel Matrix

1. INTRODUCTION

1.1 Background

The work on multi-antenna transmission techniques of early 1980s presents that a paper on wireless communications by using multiple antennas was written by Jack Winters [5] at Bell Laboratories. It presents the fundamental limits on the data rate of Multiple Input Multiple Output (MIMO) systems in case of Rayleigh fading environment. The spatial multiplexing by using MIMO was proposed by Paulraj and Kailath in 1993 [48]. In 1996, Greg Raleigh and Gerard Joseph Foschini followed the several articles of MIMO [6] and presented new approaches involving space time coding techniques to increase the spectral efficiency of multi-antenna systems. In 1999, an article [7] presents the study of MIMO Rayleigh fading link by taking information theory into account. Iospan Wireless Inc deployed first commercial MIMO system in 2001. In 2006, Broadcom and Intel introduced the new standard of wireless Local Area Network (LAN) systems named as IEEE 802.11n.

For a wide variety of applications and requirement of high data rates, the volatile evolution of MIMO systems has taken place. The technologies such as IEEE 802.11, Third Generation (3G), Universal Mobile Telecommunications System (UMTS), 3G Partnership Project (3GPP) and Long Term Evolution (LTE) depend on multi-antenna transmission techniques [1], [2], [3], [4]. Multi-antenna technology is used to increase the capacity and to improve the reliability of wireless link by deploying spatial dimension in order to integrate multiple antennas at transmitter and receiver devices.

In wireless communication systems, the recent advances [1], [2], [3], [4], [7], [8], [11], [25], [28], [29], [30], [45] have promoted the design of multi-user (MU) MIMO communication systems. The MU-MIMO systems are used for the implementation of new generation of mobile radio communication for future cellular radio standards (e.g., 3GPP LTE, Release 8 of LTE, Release 9 of LTE, and Advanced LTE, etc). 3GPP LTE exploits MU-MIMO technology and has higher spectral efficiency than existing 3G networks [8], [9]. Release 8 of LTE presents single user (SU) MIMO scheme and only uses transmission mode 5 which is defined for MU-MIMO systems. Feedback parameters such as channel rank indicator, channel quality indicator and precoding matrix indicator are required to achieve high performance of MU-MIMO systems. Release 9 of LTE is mainly improvement of Release 8. It presents transmission mode 8 and supports both SU-MIMO and MU-MIMO systems. Advanced LTE utilizes transmission mode 9 that allows possible switch between MU-MIMO and SU-MIMO.

1.2 Thesis motivation

The growing demands for higher system capacity and link throughput over limited resources introduce advanced multi-antenna techniques in wireless communication such as MU MIMO-OFDM. The advanced techniques improve wireless link reliability and spectral efficiency in future wireless systems. In MU MIMO-OFDM systems, base-station (BS) with multiple antennas communicates simultaneously with multiple users over a given time-frequency resource. Therefore, multiple radio channels are required to create link between BS and user equipment (UE). Independent fading characteristics of radio channels are achieved by deploying antenna devices on adequate apart places. In downlink (DL) transmission, BS transmits multiple data streams through its antennas towards the UE side through DL channel. In uplink (UL) transmission, UE send in parallel multiple data streams towards the BS through UL channel.

For channel estimation, two methods can be used: one with feedback and the other with reciprocity principle [24]. In feedback method, UE calculates DL channel and information is sent back to BS through UL channel. If channel is changing fast, then more frequent estimation is required. As a result, feedback method does not work appropriately. In case of reciprocity, DL and UL channels are same when time, frequency and antenna positions are same. Based on the channel reciprocity principle, the channel state information (CSI) at BS for DL transmission can be obtained through estimating the UL channel. This method works for TDD schemes because UL and DL channels work at the same frequency.

In practice, however, there are always unavoidable frequency response (FR) mismatch characteristics between transmitter and receiver. FR mismatch can thus change the reciprocal nature of DL and UL channels. Channel non-reciprocity is very challenging factor in a cellular communication MU MIMO-OFDM systems. The impact of transceiver non-reciprocity at UE causes inter-stream interference (ISI) which can be compensated using receiver signal processing. The impact of transceiver non-reciprocity at BS causes inter-user interference (IUI) that degrades the system performance of MU MIMO-OFDM systems. To ensure the system reliability and high performance in case of transceiver non-reciprocity, some non-reciprocity estimation and compensation methods are required by using precoding technique. The previous work has proposed the estimation-compensation framework [37] that gives flexible solution to restore the channel reciprocity. But there is a need to validate the findings and performance of the proposed estimation-compensation framework. It has motivated the modeling of transceiver FR mismatch characteristics using actual measurement data in this research work in order to prove the validation of the earlier used approach.

1.3 Research objective

The research objective of this research work is to model the FR mismatch parameters at BS in order to improve the performance of MU MIMO-OFDM DL transmission systems using actual measurement data.

The thesis work consists of different stages. In the first stage, non-reciprocity matrices at BS and UE are extracted from measurement data. During the second stage, the impact of transceiver non-reciprocity extracted from measurement data is analyzed in the TDD precoded MU MIMO-OFDM system. In the third stage, the system performance in case of non-reciprocity is compensated (close to ideal precoded MU MIMO-OFDM system) by estimating non-reciprocity parameters at BS.

1.4 Author contribution

The major contributions of the thesis are described in this section. The literature review has been carried out by studying the basic communication systems and fundamental concepts of MIMO, OFDM, SU MIMO-OFDM and MU MIMO-OFDM systems covering linear precoding and channel coding schemes.

Extraction of non-reciprocity parameters from measurement data is carried out in order to model FR mismatch parameters at BS and UE through signal modeling using mathematics. The simulator has been implemented to extract FR mismatch parameters. Then, the achieved characteristics of the FR mismatches are analyzed.

The simulator has been implemented in order to demonstrate impact of measured transceiver non-reciprocity using ZF precoding. The analysis of the achieved results has been presented using both error control coded and uncoded channels.

The simulator has been implemented to estimate the transceiver non-reciprocity matrix at BS for compensation of the transceiver non-reciprocity. In case of compensated non-reciprocity using uncoded and coded channel, the interpretation of the simulation results has been illustrated.

1.5 Thesis outline

The rest of the thesis comprises of five chapters. Chapter 2 contains the theoretical background of MIMO, OFDM, SU MIMO-OFDM and MU MIMO-OFDM techniques. Chapter 3 presents the extraction method of non-reciprocity parameters at BS and UE from measurement data along with obtained results. Chapter 4 explains the impact of extracted non-reciprocity parameters in the TDD precoded MU MIMO-OFDM system including simulated results. Chapter 5 describes the compensation method in order to achieve better performance by using pilot-based estimation of non-reciprocity parameters

at the transceiver of BS. This chapter also illustrates the results for estimation performance and compensated non-reciprocity performance. The conclusion and the work related to future are presented in Chapter 6.

2. MIMO AND OFDM BASICS

In this chapter, the basic fundamentals of MIMO, OFDM, and SU MIMO-OFDM systems are presented. MU MIMO-OFDM system is explained covering precoded technique for DL transmission.

2.1 MIMO systems

In MIMO systems, more than one antenna configuration is deployed in transmitter and receiver for wireless radio communication. It is basically extensive approach in the development of antenna array communication. MIMO techniques have been proposed by the researchers [31], [39], [40], [41] and these techniques are extensively used in the development of advanced wireless systems [1], [2], [3], [4]. In MIMO technology, spatial multiplexing, spatial diversity and antenna array beam-forming are used as gain mechanisms. Spatial multiplexing [39], [40], [43], [44] increases the spectral efficiency of wireless link in the rich scattering environment that provides multiplexing gain. Spatial diversity [39], [42], [43] improves the link reliability by transmitting the signal on independent fading branches which gives diversity gain. The directional properties (efficient utilization of radiated power from antenna) are created by using antenna array beam-forming that gives array gain.

There are numerous MIMO configurations. $N_r \times N_t$ MIMO configuration denotes that system has N_t antennas that are used to transmit signals from transmitter and N_r antennas that are used to receive signals at receiver. The general model of MIMO system is represented in Figure 2.1.
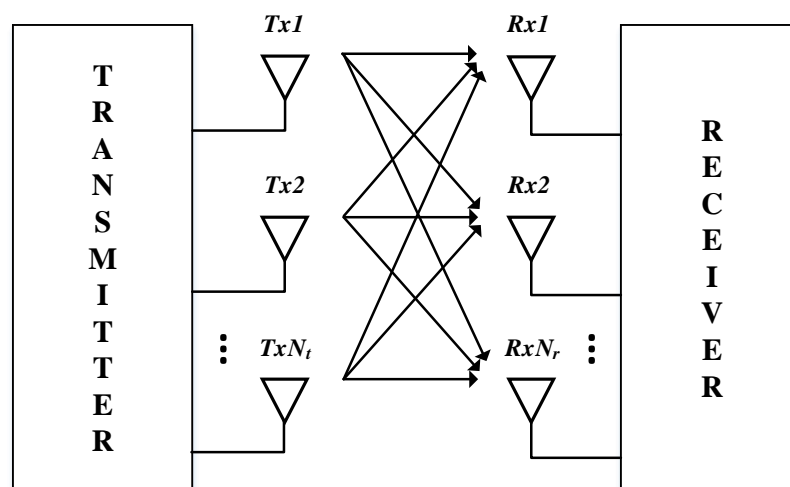

Figure 2.1. *General model of MIMO system*

The flat fading channel model for MIMO system is defined as:

$$y = \mathbf{H}.x + n \tag{1}$$

Where y is a complex received signal vector at receiver, x is a complex transmitted signal vector from transmitter and n is a complex additive noise signal vector. The transmitter and receiver consist of antennas $Tx1$, $Tx2$,..., TxN_t and $Rx1$, $Rx2$,..., RxN_r respectively. The transmitted signal vector x comprises of independent data sub-streams. The receiver recombines the transmitted sub-streams. The transmitted vector x and received vector y are as under:

$$x = \begin{bmatrix} x_1 & x_2 & \cdots & x_{N_t} \end{bmatrix}^T \tag{2}$$

$$y = \begin{bmatrix} y_1 & y_2 & \cdots & y_{N_r} \end{bmatrix}^T \tag{3}$$

The MIMO channel matrix for $N_r \times N_t$ MIMO system is described in equation (4), where $\mathbf{H}$ is ($N_r \times N_t$) complex channel matrix.

$$\mathbf{H} = \begin{pmatrix} h_{11} & h_{12} & \cdots & h_{1N_t} \\ h_{21} & h_{22} & \cdots & h_{2N_t} \\ \vdots & \vdots & \ddots & \vdots \\ h_{N_r 1} & h_{N_r 2} & \cdots & h_{N_r N_t} \end{pmatrix} \tag{4}$$

MIMO gives efficient usage of spectral bandwidth by catering the spatial diversity which provides greater capacity. The theoretical channel capacity defined by Shannon-Hartley is:

$$C = BW \log_2(1 + SNR) \tag{5}$$

Where C denotes channel capacity, BW is signal bandwidth and SNR represents signal-to-noise ratio. By increasing channel's SNR, a marginal gain in channel throughput is achieved as expressed in equation (5). Higher data rates can be achieved with the increase of signal bandwidth. But higher signal bandwidth increases its susceptibility to multipath fading. When channel is affected by interference or multipath fading, it will change the bit error rate (BER) with respect to SNR. Therefore, OFDM is used in combination with MIMO technique in order to work well in case of multipath fading.

MIMO technology gives LOS and NLOS performance improvement. By increasing the gain of antenna array, SNR is improved. Link spectral efficiency is increased by using

phase nulling techniques. Throughput is improved due to parallel data channelization (i.e., ability to provide high data rate compared to range). Multi-antenna techniques give improved performance in the presence of interference, multipath signal fading. Capacity is also enhanced linearly with the increase of number of transmit and receive antennas. MIMO supports both TDD and FDD techniques.

The disadvantages include need of multiple antennas, implementation complexity and antenna cost.

2.2 OFDM modulation

In 1960s and 1970s, orthogonal frequency-division multiplexing (OFDM) was considered during investigation of diminishing interference between channels in frequency domain [19]. OFDM has been used extensively in wireless communication systems such as digital video broadcasting systems, digital audio broadcasting systems, digital subscriber line standards, wireless broadband access standards (e.g.,WiMAX), wireless LAN standards (e.g., 802.11a/g and HIPERLAN2) and 4G wireless mobile communications because of higher data rate transmission ability and its robustness due to delay and multipath fading [17], [18], [20].

OFDM technique supports high speed data transmission over wireless links in case of delay spread, inter-symbol interference (ISI), fading and random phase distortion. Such problems are encountered when signal follows several propagation paths and the paths reach the receiver with different propagation delays.

OFDM is a scheme of digital modulation in which high rate data stream is divided into small parallel sub-streams of reduced data rate transmitted over separate subcarriers. In brief, it is a type of multicarrier digital communication technique. Figure 2.2 represents the comparison between multicarrier and single carrier transmission. In single carrier transmission, only one radio frequency carrier is used to carry information of input data. Whereas, multi-carrier or OFDM system uses multiple carriers with different carrier frequencies.

If carrier frequencies are uniformly distributed in frequency domain by frequency spacing, $f_s = 1/(NT_s)$, then the OFDM signal is given in equation (6). Where, X_l is complex value at l^{th} subcarrier to be transmitted. If constant (1/N) is not multiplied, then equation corresponds to N-point IFFT.

$$x(nT_s) = \sum_{l=0}^{N-1} X_l e^{j2\pi nl/N} \tag{6}$$
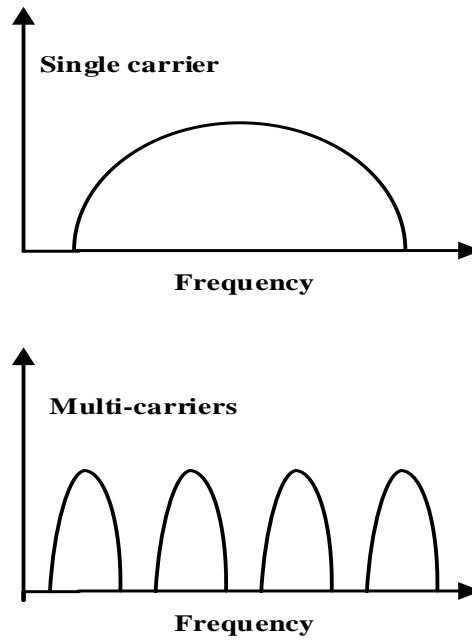
Figure 2.2. *Comparison between multi-carriers and single carrier*

Frequency division multiplexing (FDM) is a technology that is basis of OFDM. It uses multiple frequencies to simultaneously transmit multiple signals in parallel. Each signal has its own frequency range (subcarrier) and detached by guard space to confirm that subcarriers do not overlap. In case of OFDM, it is more efficient by spacing the subcarriers much closer so that overlapping takes place. It is carried out by selecting frequencies that are orthogonal. It allows the spectrum of each subcarrier to overlap another without interfering with it. Figure 2.3 shows the comparison of FDM and OFDM technique.

Figure 2.3. *Comparison between OFDM and FDM*

The block diagram of OFDM system is presented in Figure 2.4. OFDM transmitter comprises of data mapping, IFFT, insertion of cyclic prefix (CP) and parallel-to-serial (P/S) convertor. The same steps are followed in the receiver but in reverse order such as serial-to-parallel (S/P), CP removal, FFT and de-mapping of data. To eliminate ISI, CP is used as a guard interval at the start of each OFDM symbol. OFDM is the exploitation of orthogonal principle of m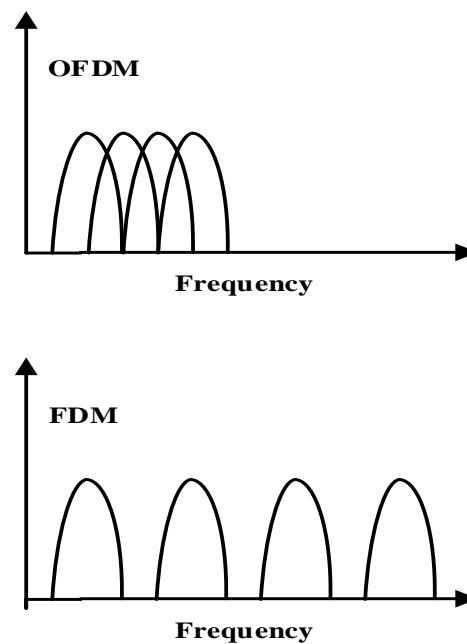athematics because it enables receivers to separate the subcarriers via an FFT and eliminate the guard bands. OFDM subcarriers can overlap to make full use of the spectrum. But at the peak of each subcarrier spectrum, the power in all the other subcarriers is zero.
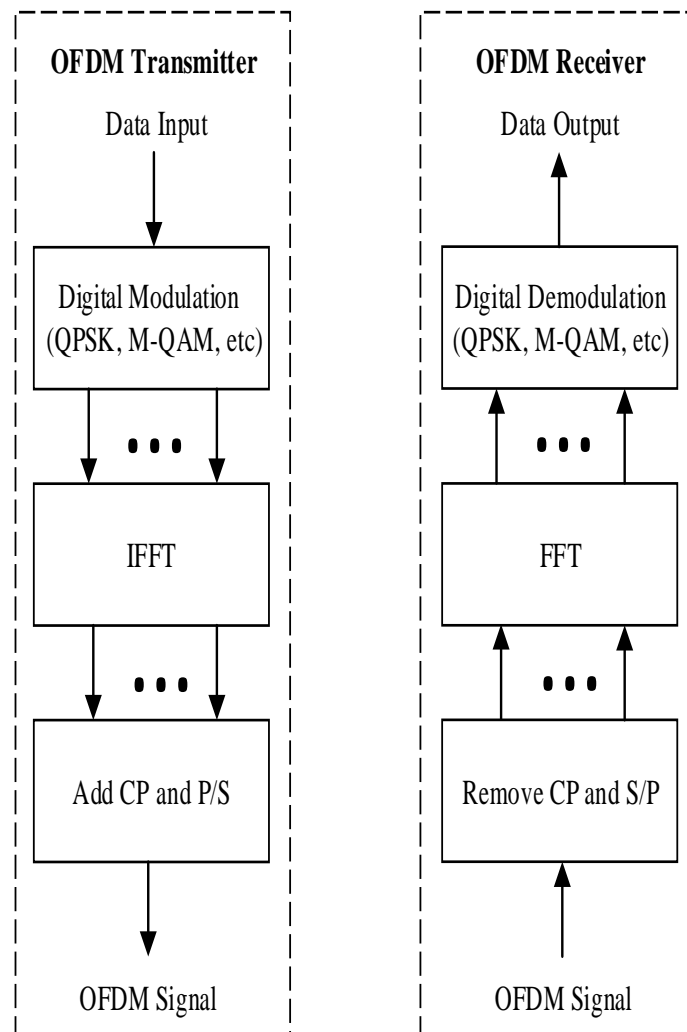
Figure 2.4. OFDM system model

The advantages of OFDM technique include that OFDM is more robust against frequency selective fading or multipath fading. It gives higher spectral efficiency and possesses interference suppression capability. It provides simple digital implementation by means of IFFT/FFT operations. It enhances protection against narrow band interference. Adaptive data rate per subcarrier can be achieved to enhance capacity of the system. The drawbacks of OFDM over single carrier include that it is sensitive to frequency and phase noise. It has inherent loss in spectral efficiency related to use of CP.

Power amplifiers are required for linear behavior due to high peak to average power ratio (PAPR) characterization in OFDM systems.

2.3 SU MIMO-OFDM

Traditional MIMO-OFDM system is usually referred as SU MIMO-OFDM. It is also known as point-to-point MIMO-OFDM. In SU MIMO, BS communicates with only one UE. Both BS and UE are equipped with number of antennas.

The main motivation behind the development of MIMO-OFDM in broadband wireless communication systems is to provide higher data rates over longer distances. MIMO systems have its susceptibility due to multipath fading. Therefore, OFDM technique is used to alleviate multipath problem by using either TDD or FDD multiplex schemes. By combining both MIMO and OFDM techniques, it gives extremely beneficial results such as link reliability in highly obstructive environment, high spectral coverage, high data rates up to hundreds of MB and greater channel capacities. MIMO-OFDM takes advantage of the multipath properties using BS antennas that do not have LOS channel. By combining both techniques, it provides high throughput and robustness [23].

In Figure 2.5, OFDM modulator is used to modulate the data at transmitter side and then data signals are transmitted by MIMO system through all N_t antennas. At the receiver of MIMO-OFDM system, the data signals are received through all N_r antennas and recovered by using OFDM demodulator.
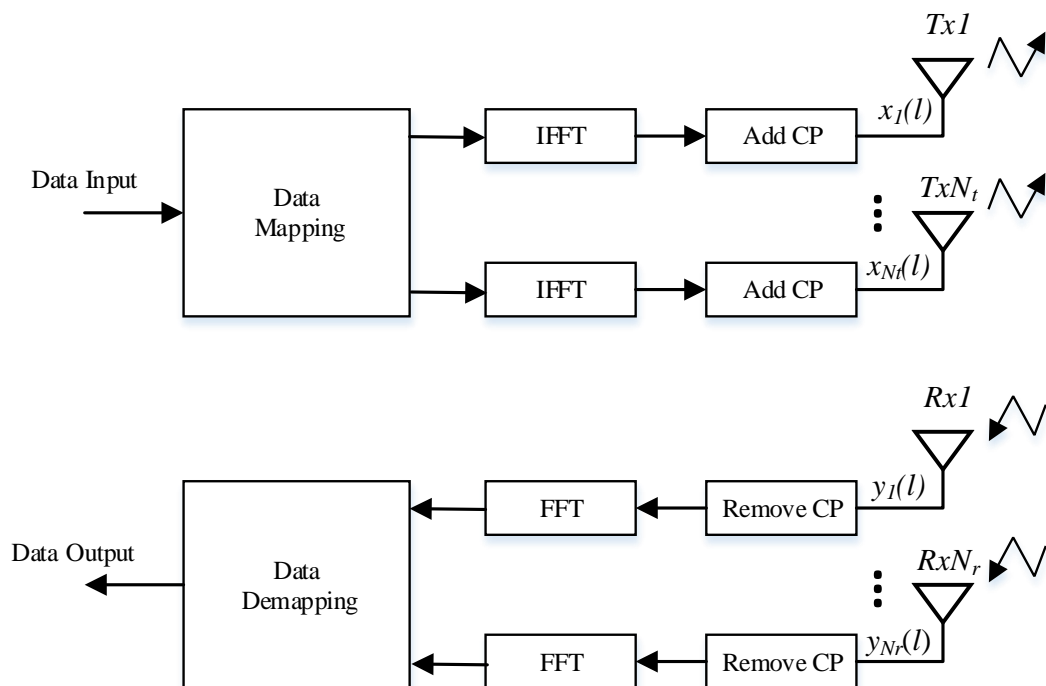

Figure 2.5. *SU MIMO-OFDM system*

The channel model for MIMO-OFDM system is defined as:

$$y(l) = \mathbf{H}(l).x(l) + n(l) \tag{7}$$

$y(l)$ is complex received signal vector at l^{th} subcarrier at the receiver, $x(l)$ is complex transmitted signal vector at l^{th} subcarrier from transmitter and $n(l)$ is complex additive noise signal vector at l^{th} subcarrier. The transmitted signal vector $x(l)$ that comprises of independent data sub-streams at l^{th} subcarrier is given as:

$$x(l) = \begin{bmatrix} x_1(l) & x_2(l) & \cdots & x_{N_t}(l) \end{bmatrix}^T \tag{8}$$

The receiver recombines the transmitted sub-streams. The received signal vector at l^{th} subcarrier is as under:

$$y(l) = \begin{bmatrix} y_1(l) & y_2(l) & \cdots & y_{N_r}(l) \end{bmatrix}^T \tag{9}$$

In case of MIMO-OFDM, the channel matrix for $N_r \times N_t$ MIMO system is described as follows:

$$\mathbf{H}(l) = \begin{pmatrix} h_{11}(l) & h_{12}(l) & \cdots & h_{1N_t}(l) \\ h_{21}(l) & h_{22}(l) & \cdots & h_{2N_t}(l) \\ \vdots & \vdots & \ddots & \vdots \\ h_{N_r 1}(l) & h_{N_r 2}(l) & \cdots & h_{N_r N_t}(l) \end{pmatrix} \tag{10}$$

Where $\mathbf{H}(l)$ is ($N_r \times N_t$) complex channel matrix over l^{th} subcarrier. Multi-antenna communication techniques make OFDM as a leading transmission technique in wireless LAN. Because of greater spectral efficiency, it can be used in new applications and allows more cost-effective implementation for existing applications.

2.4 MU MIMO-OFDM

In contrast to SU MIMO-OFDM systems, many users communicate with a BS in the case of multi-user MIMO systems over a given time-frequency resource. MU MIMO-OFDM system becomes even more interesting because it provides an additional opportunity to exploit new communication systems due to many users [10]. These systems are proposed to improve the rate of communication while keeping the same level of reliability. The simultaneous communication of multiple users over the same spectrum improves the system performance [25]. The main advantage is that multiplexing gain is achieved. Moreover, the performances of MU-MIMO and SU-MIMO systems in terms of throughput depend on the SNR level. SU MIMO-OFDM systems perform better at lower values of SNR. However, MU MIMO-OFDM systems provide better performances at

higher values of SNR. MU MIMO-OFDM systems require perfect CSI in order to achieve high throughput and to improve the multiplexing gain in contrast to SU MIMO-OFDM systems.

Generalized MU-MIMO systems may comprise of more than one BS where different number of antennas could be deployed. In case of different number of stations, the BS can also be operated through cooperation by establishing link between them [25]. In this research, the work is carried out for one BS and two UE devices. Therefore, MU-MIMO with single BS is illustrated in detail.

Figure 2.6 presents MU-MIMO system in which one BS (equipped with $Tx_1,\ldots, Tx_{N_t}$ antennas) communicates with user 1 (equipped with $Rx_1,\ldots, Rx_{N_{r_1}}$ antennas) to user K (equipped with $Rx_1,\ldots, Rx_{N_{r_K}}$ antennas) respectively.
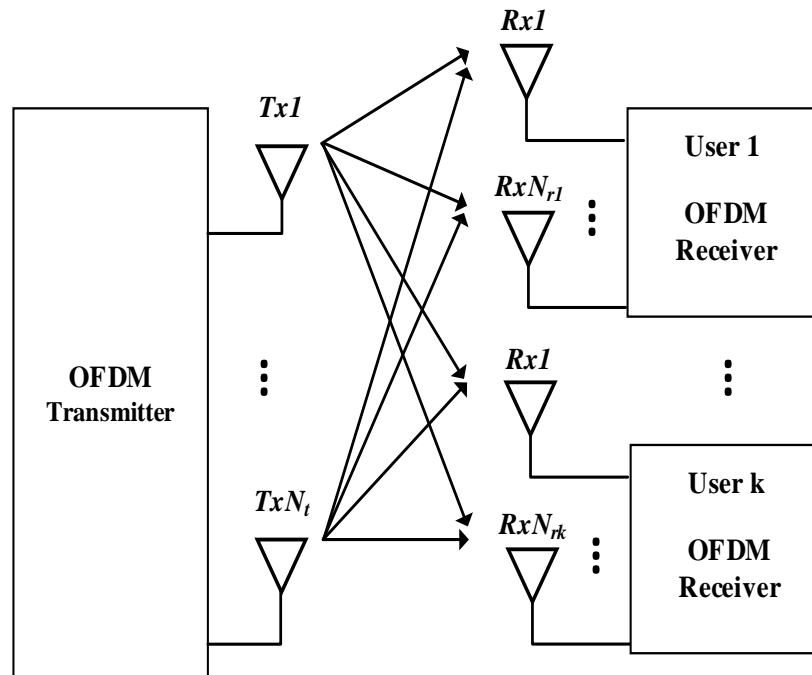
Figure 2.6. MU-MIMO system model

Communication schemes include both UL MU-MIMO and DL MU-MIMO in MU-MIMO OFDM systems. The DL communication in case of MU MIMO-OFDM system is represented in Figure 2.6. In case of UL communication, users send signals to BS.

The drawback of MU-MIMO includes strong co-channel interference. In order to solve the problem of interference in MU-MIMO systems, different approaches have been proposed for interference management [26], [27]. Some of these approaches are based on beam-forming technique [28]. The DL MU MIMO-OFDM system can use linear precoding techniques. There are different types of precoding techniques such as ZF and

block diagonalization [36]. In this research work, ZF precoding technique has been used in order to suppress IUI.

2.4.1 Zero-forcing (ZF)

ZF precoding is low complexity technique [15], [16], [45], [46] that is used in the transmitter side in order to null or suppress the multi-user interference in MU MIMO-OFDM communication systems. The purpose of this solution is to improve the sum rate capacity of the communication system under the given power constraint. Such type of performance can be attained by canceling IUI.

The ZF precoder is formulated as:

$$\mathbf{W} = \mathbf{H}_{DL}^T (\mathbf{H}_{DL} \mathbf{H}_{DL}^T)^{-1} \tag{11}$$

$\mathbf{H}_{DL}$ is a Rayleigh fading multipath DL channel matrix. $\mathbf{W}$ is precoded matrix that is acquired by using channel matrix. In case of ZF precoding, each transmitted symbol to the user K antenna is precoded by a vector which is orthogonal to the columns of channel matrix $\mathbf{H}_{DL,K}$ [25]. The precoded data vector can be written as follow:

$$x(l) = \mathbf{W}(l)s(l) \tag{12}$$

$x(l)$ is precoded data, $s(l)$ is transmitted signal for user K and $\mathbf{W}(l)$ is precoded matrix at l^{th} subcarrier of the MU MIMO-OFDM system. The receiver input vector for user K at l^{th} subcarrier is obtained in equation (13) after experiencing MIMO radio multipath from BS to user K.

$$r_K(l) = \mathbf{H}_{DL,K}(l)x(l) + n_K(l) \tag{13}$$

$$r_K(l) = \mathbf{H}_{DL,K}(l)\mathbf{W}(l)s(l) + n_K(l) \tag{14}$$

$\mathbf{H}_{DL,K}(l)$ refers downlink channel at l^{th} subcarrier for user K and $n_K(l)$ is noise vector at l^{th} subcarrier for user K receiver. The transmission channel used for data precoding is given as:

$$\mathbf{H}_T(l) = \mathbf{H}_{DL,K}(l)\mathbf{W}(l) \tag{15}$$

The transmission channel matrix satisfies $\mathbf{H}_T(l) = \mathbf{I}$ in case of reciprocity and $\mathbf{H}_T(l) \neq \mathbf{I}$ in case of non-reciprocity. This method guarantees that the impact of other user streams is cancelled at the target receiver.

2.4.2 TDD and reciprocity

The CSI at BS is required for multi-user precoding in the DL and detection in the UL in MU MIMO-OFDM systems. The channel estimation in MIMO systems requires frequency or time resource that is associated to the number of antennas at BS [29].

In case of frequency division duplex (FDD) scheme, both UL and DL channels use different frequency bands. The CSI required for UL and DL channels is also different. FDD utilizes feedback and can be used as paired scheme. On the other hand, the reciprocity principle does not require feedback. Therefore, TDD scheme gives beneficial characteristics in case of reciprocity principle in multi-antenna BS systems.

For MU MIMO-OFDM systems, the approach that can be used to sort out the reciprocity problem is channel estimation in TDD systems. According to the channel reciprocity principle, only UL channel needs to be estimated. In TDD system [30], the users send UL data with pilot sequences to BS and then BS estimates CSI to users by using pilot sequences. Then, BS detects UL data by utilizing estimated CSI and sends data for DL transmission by using precoding method. The real advantage of TDD is that it only needs a single channel of frequency spectrum. The only problem is that specific timing and synchronization system is required at BS and UE devices.

3. MODELING OF NON-RECIPROCITY

The modeling of channel reciprocity plays an important role in wireless communication systems. The FR mismatches between BS and UE transceivers can exist even if good antenna isolation in each device is presumed. FR mismatches mismatch can thus change the reciprocal nature of DL and UL channels. As a result, the performance of MIMO systems is degraded. In order to improve performance, the behavior of FR mismatches should be determined first at BS and UE. Therefore, the FR mismatches at BS and UE transceivers are extracted by using measurement data.

3.1 Modeling of FR mismatches from measurement data

3.1.1 Measurement setup

The actual measurement data setup, used in this work, comprises of one BS with two antennas and two mobile station (MS) devices having single antenna as shown in Figure 3.1 and Figure 3.2. $Tx1$ and $Tx2$ are two antennas at BS and $Rx1$ and $Rx2$ are two antennas at both users respectively. The five line-of-sight (LOS) measurements were carried out at short distances (a few meters) in a corridor. In each batch, two frames were transmitted from BS to MS in case of DL transmission and MS to BS in case of UL transmission. The time between the consecutive frames was 40ms. MS position is changed by several wavelengths in each batch. The simulation specifications used in the measurement data are shown in Table 3-1.

Table 3-1. *Simulation specifications*

Parameters	Values
MIMO Configuration	2×2
OFDM Symbols	20
Pilot Subcarriers	2
FFT Size	80
Subcarriers	38
Modulation	64-QAM
Channel	LOS
Standard	802.11a
Subcarrier Spacing	312.5kHz
Sampling Frequency	25MHz

In measurement data, MU MIMO-OFDM simulator generates 2×2 channel matrices corresponding to all subcarriers from BS to both MS (DL channel matrix is represented by $\mathbf{H}_{DL}$) and from both MS to BS (UL channel matrix is represented by $\mathbf{H}_{UL}$). From Figure 3.1 and Figure 3.2, DL and UL channel matrices can be written as:

$$\mathbf{H}_{DL} = \begin{bmatrix} h_{11} & h_{12} \\ h_{21} & h_{22} \end{bmatrix} \tag{16}$$

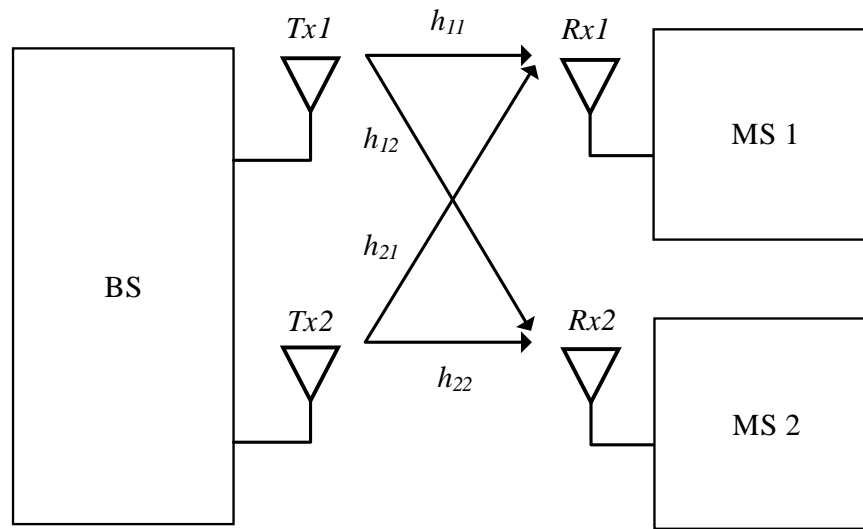$$\mathbf{H}_{UL} = \begin{bmatrix} h_{11} & h_{21} \\ h_{12} & h_{22} \end{bmatrix} \tag{17}$$

Figure 3.1. *Downlink transmission in case of two MS devices*
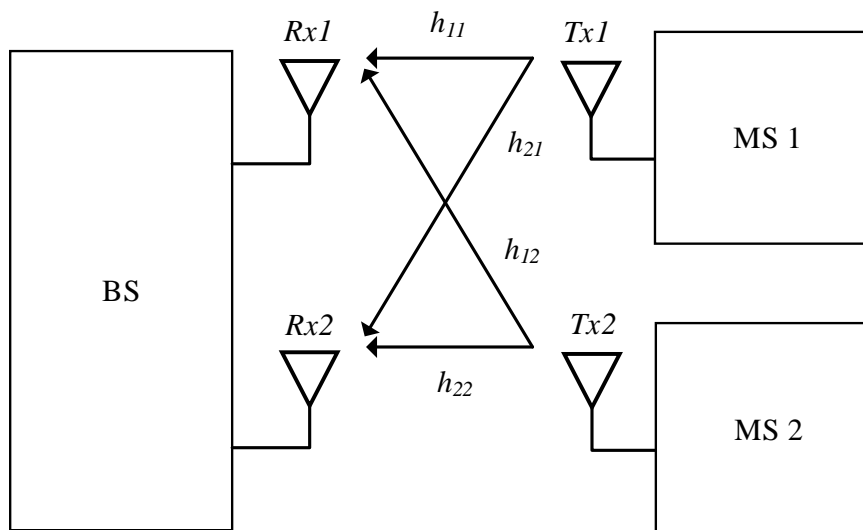

Figure 3.2. *Uplink transmission in case of two MS devices*

3.1.2 Parameters extraction procedure

In TDD system, the CSI at BS for DL channel can be determined by measuring UL channel at same operating frequency. Thus, ideally it can be written as:

$$\mathbf{H}_{UL} = \mathbf{H}_{DL}^{T} \tag{18}$$

In practice, the DL and UL channels have some unavoidable FR mismatches due to electronic components used in the communication devices. Therefore:

$$\mathbf{H}_{UL} \neq \mathbf{H}_{DL}^{T} \tag{19}$$

$$\mathbf{H}_{UL} = \mathbf{A}_{b} \, \mathbf{H}_{DL}^{T} \mathbf{A}_{u} \tag{20}$$

The non-reciprocity matrices at BS and UE are represented by $\mathbf{A}_{b}$ and $\mathbf{A}_{u}$ respectively and can be written as:

$$\mathbf{A}_{b} = \begin{bmatrix} n_{1} & 0 \\ 0 & n_{2} \end{bmatrix} \tag{21}$$

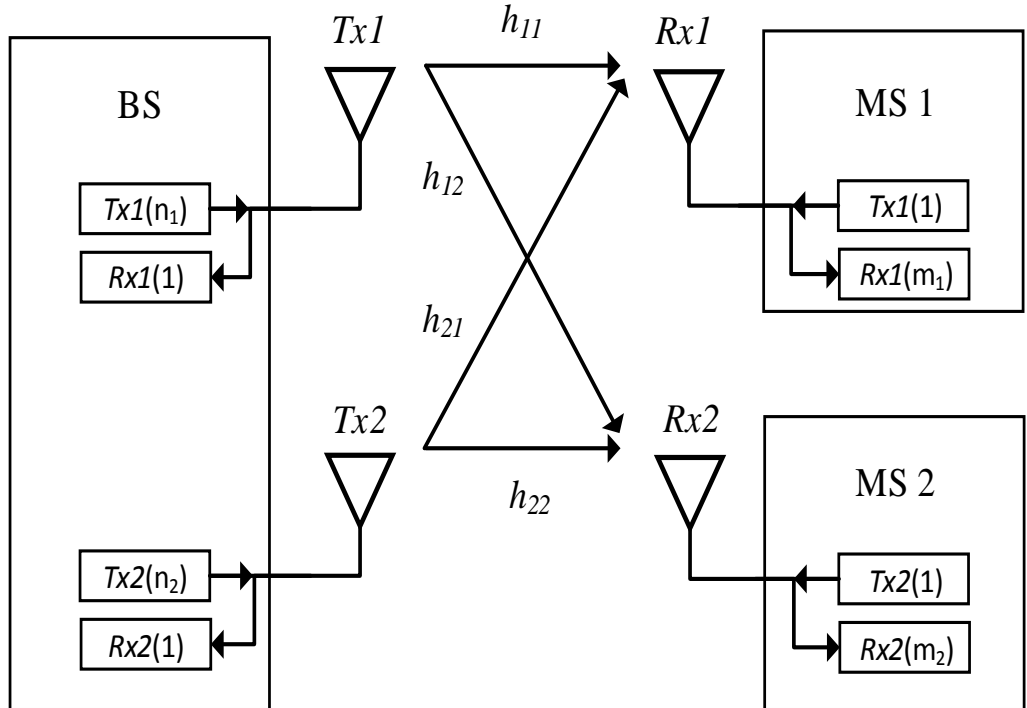$$\mathbf{A}_{u} = \begin{bmatrix} m_{1} & 0 \\ 0 & m_{2} \end{bmatrix} \tag{22}$$

Figure 3.3. *Downlink transmission including FR mismatches*

The coefficients n_1 and n_2 denote the FR mismatches at BS transmitting antennas $Tx1$ and $Tx2$ respectively. Similarly, m_1 and m_2 indicate FR mismatches at receiving antennas of MS1 and MS2 respectively as shown in Figure 3.3. From equation (20), we can write in terms of FR mismatch coefficient for individual user as under:

$$\begin{bmatrix} h_{11}^{UL} \\ h_{12}^{UL} \end{bmatrix} = \begin{bmatrix} n_1 & 0 \\ 0 & n_2 \end{bmatrix} \begin{bmatrix} h_{11}^{DL} \\ h_{21}^{DL} \end{bmatrix} m_1 \tag{23}$$

$$\begin{bmatrix} h_{21}^{UL} \\ h_{22}^{UL} \end{bmatrix} = \begin{bmatrix} n_1 & 0 \\ 0 & n_2 \end{bmatrix} \begin{bmatrix} h_{12}^{DL} \\ h_{22}^{DL} \end{bmatrix} m_2 \tag{24}$$

The DL channel between $Tx1$ and $Rx1$ is represented by h_{11}^{DL} and UL channel between $Rx1$ and $Tx1$ is denoted by h_{11}^{UL} and so on. From equation (23) and (24), FR mismatch values are determined as given below:

$$n_1 m_1 = \frac{h_{11}^{UL}}{h_{11}^{DL}} ; n_2 m_1 = \frac{h_{12}^{UL}}{h_{21}^{DL}} \tag{25}$$

$$n_1 m_2 = \frac{h_{21}^{UL}}{h_{12}^{DL}} ; n_2 m_2 = \frac{h_{22}^{UL}}{h_{22}^{DL}} \tag{26}$$

Where $n_1 m_1$ denotes the FR mismatch value between $Tx1$ and $Rx1$. $n_2 m_1$ denotes the FR mismatch value between $Tx2$ and $Rx1$. $n_1 m_2$ denotes the FR mismatch value between $Tx1$ and $Rx2$. Similarly, $n_2 m_2$ denotes the FR mismatch value between $Tx2$ and $Rx2$.

From measurement data, we can only extract values of $n_1 m_1$, $n_2 m_1$, $n_1 m_2$, and $n_2 m_2$ instead of n_1, n_2, m_1, and m_2 due to two linear equations and four unknowns. To extract the individual values for non-reciprocity matrix at BS and UE, a few steps are proposed. First, the FR mismatch ratios $\frac{n_1 m_1}{n_2 m_1}$, $\frac{n_1 m_2}{n_2 m_2}$, $\frac{n_1 m_1}{n_1 m_2}$, and $\frac{n_2 m_1}{n_2 m_2}$ are computed subcarrier-wise from equations (25) and (26).

Figure 3.4 shows the subcarrier-wise FR mismatches which are computed using equations (25) and (26). The responses of ratios over subcarriers are also shown in Figure 3.5.
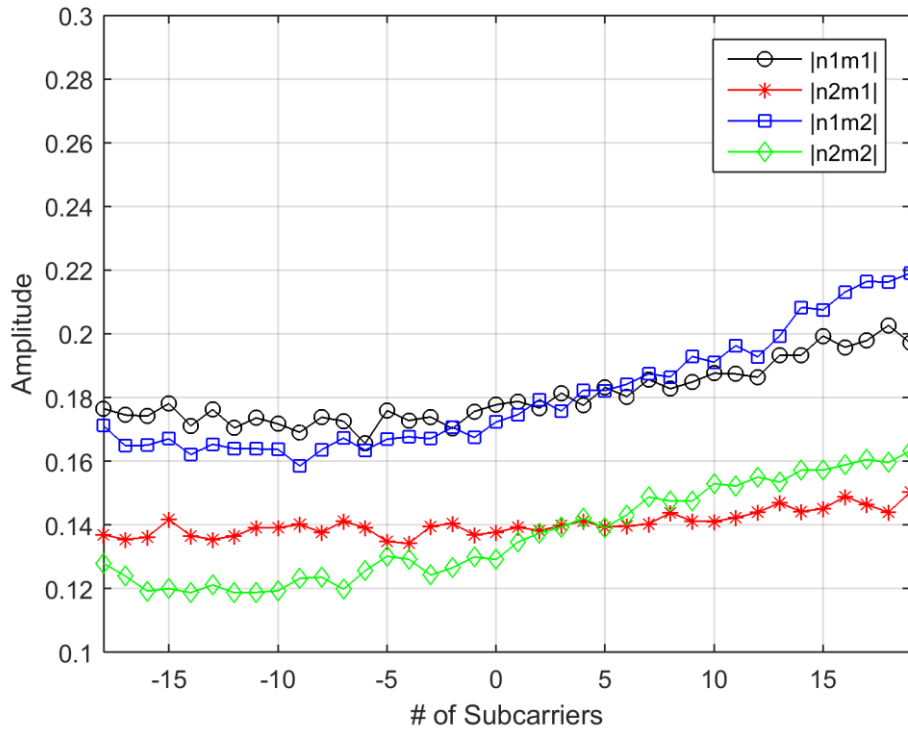
Figure 3.4. *FR mismatches from measurement data*
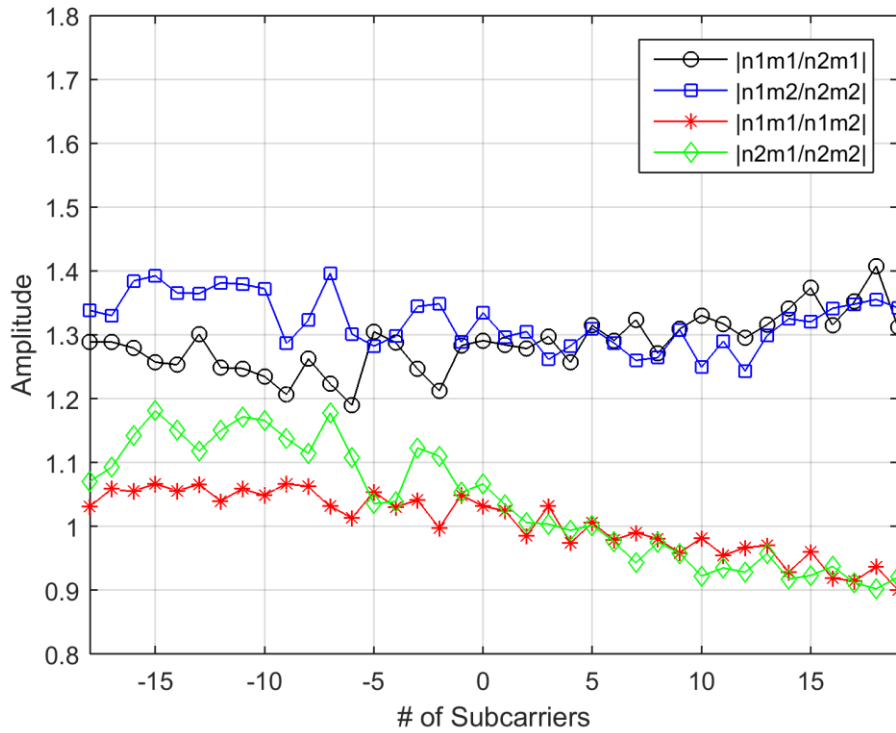
Figure 3.5. *Ratios of FR mismatch values*

Figure 3.6 shows the average response of ratios in terms of $\left|n_1 / n_2\right|$ and $\left|m_1 / m_2\right|$ at BS and UE respectively for all subcarriers.

Figure 3.6. *Ratios of FR mismatch values after averaging (frequency response)*

The time-domain signals for FR mismatch ratios in terms of $\left|n_1 / n_2\right|$ and $\left|m_1 / m_2\right|$ are shown in Figure 3.7.

Figure 3.7. *Ratios of FR mismatch values after averaging (time response)*

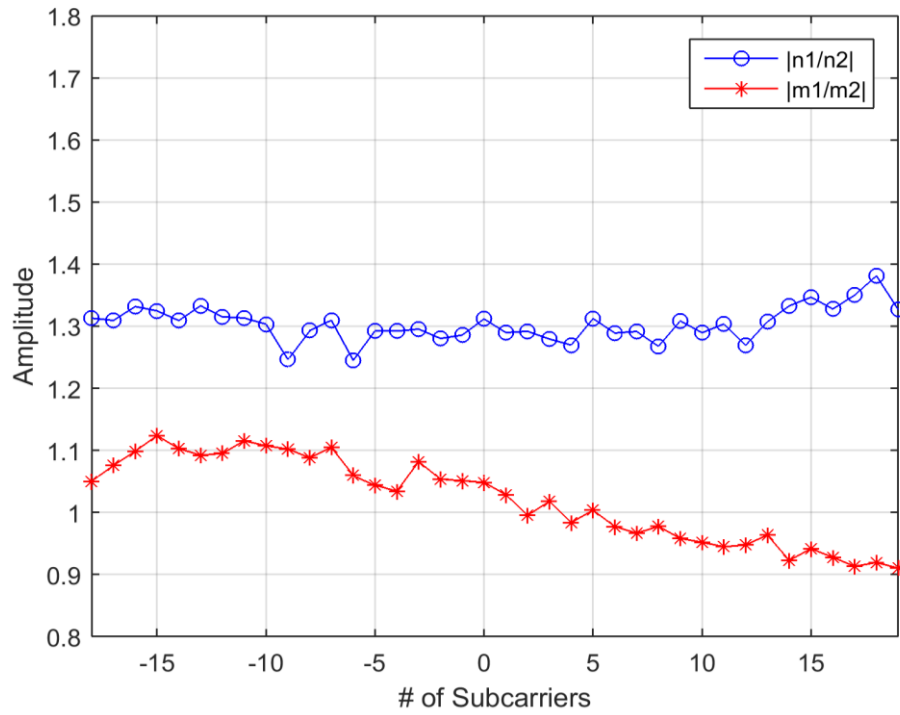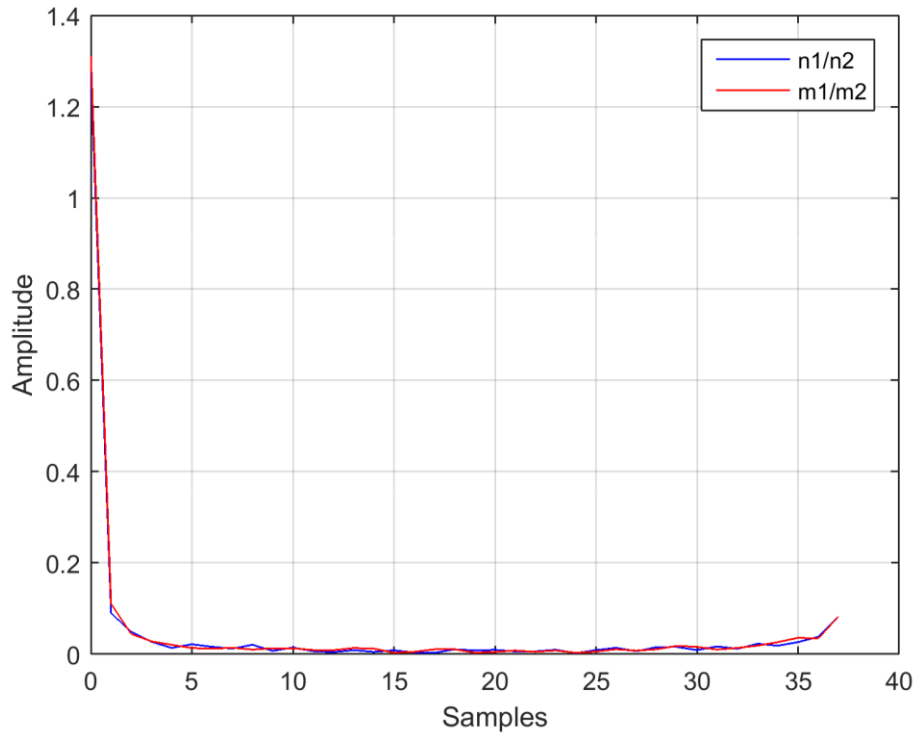The nulling technique is applied on ratios of FR mismatch coefficients and computed signals (approximated) by nulling the taps that are approximately equal to zero. When original and approximated signals are equivalent, then the mean of the signal corresponds to 1.

$$x = R_o . R_a^{-1} \Rightarrow \sum_{l=1}^{N} x_l \approx 1 \tag{27}$$

R_o is original ratio of n_1 / n_2 or m_1 / m_2 and R_a is approximated ratio of n_1 / n_2 or m_1 / m_2 respectively after applying nulling technique. N denotes the total number of subcarriers. The time, frequency and phase responses of approximated signals in terms of n_1 / n_2 at BS and m_1 / m_2 at UE are shown in Figure 3.8, Figure 3.9 and Figure 3.10 respectively. The difference between the original and approximated signals with respect to mean is shown in Table 3-2.

Table 3-2. *Comparison of real and approximated signals*

Coefficient Ratios	Mean	Difference
n_1 / n_2	1.0003	7.9774e-04

m_1 / m_2	1.0004	8.2277e-04
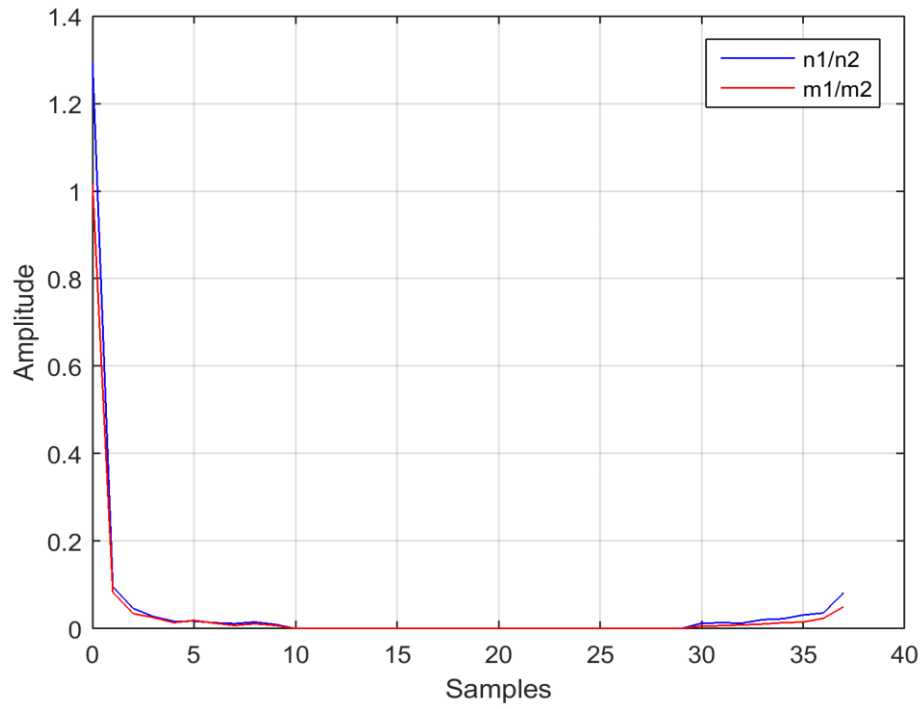
Figure 3.8. *Ratios of FR mismatch values using nulling technique (time response)*
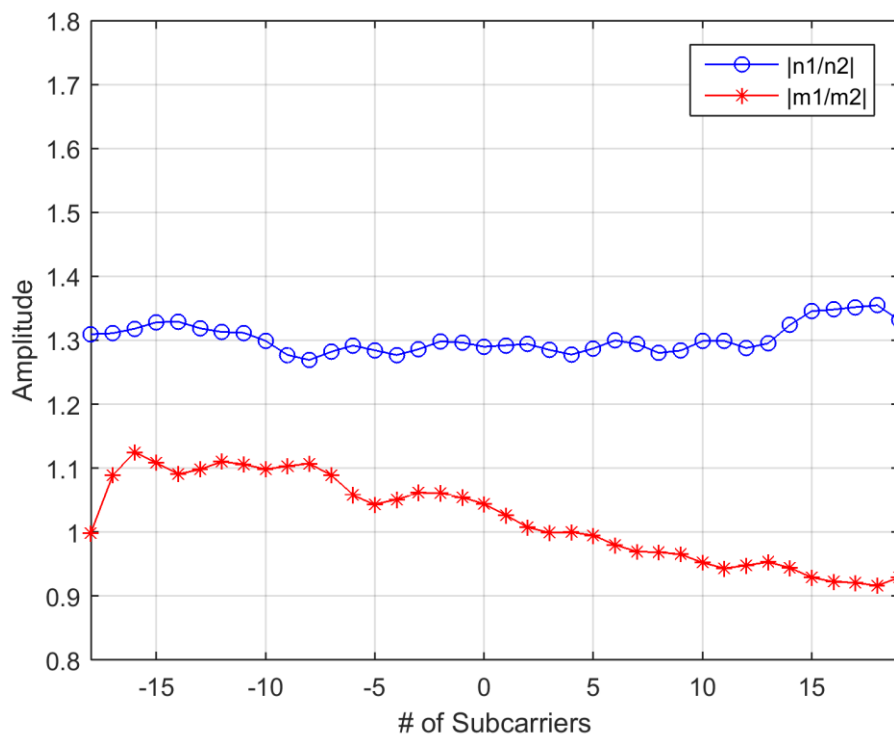
Figure 3.9. *Ratios of FR mismatch values using nulling technique (frequency response)*

Figure 3.10. *Ratios of FR mismatch values using nulling technique (phase response)*

After this, normalized values are determined for n_1, n_2, m_1 and m_2 from ratios. The normalized values are extracted in this way that the average power distribution between the normalized parameters is set to 1. The normalized FR mismatch parameters at BS are computed as under:

$$\hat{n}_1 = \frac{1}{\sqrt{1 + |n_2/n_1|^2}} \tag{28}$$

$$\hat{n}_2 = \frac{e^{j(\varphi_{n2} - \varphi_{n1})}}{\sqrt{1 + |n_1/n_2|^2}} \tag{29}$$

The time, frequency and phase responses of normalized FR mismatch parameters at BS over subcarriers are shown in Figure 3.11, Figure 3.12 and Figure 3.13 respectively.

Figure 3.11. *Extracted parameters ($\hat{n}_1$ and $\hat{n}_2$) at BS (time response)*
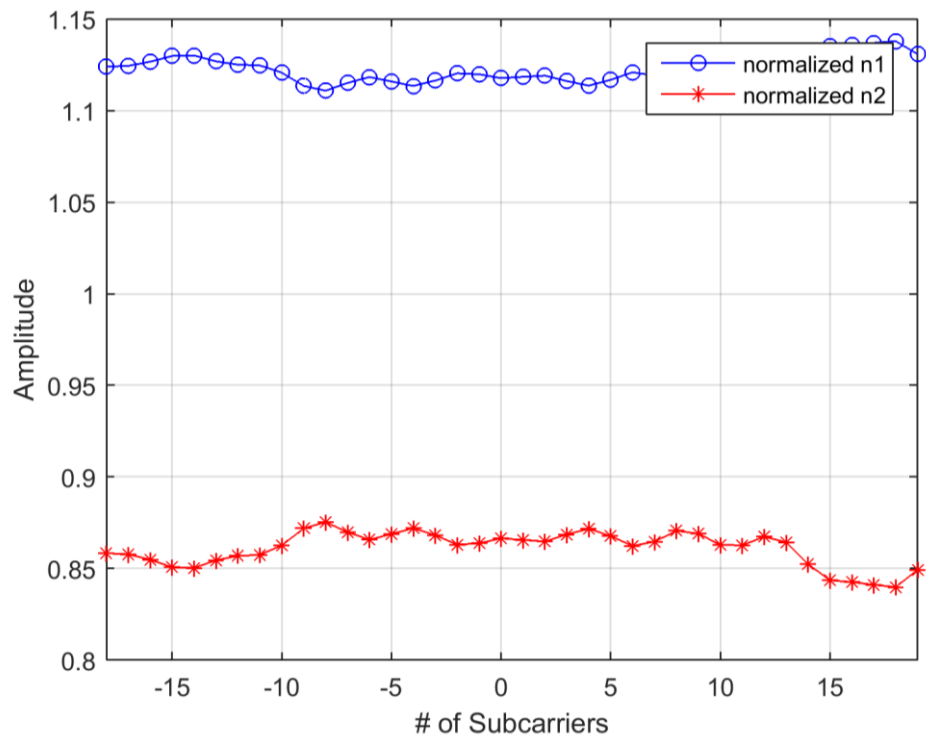
Figure 3.12. *Extracted parameters ($\hat{n}_1$ and $\hat{n}_2$) at BS (frequency response)*
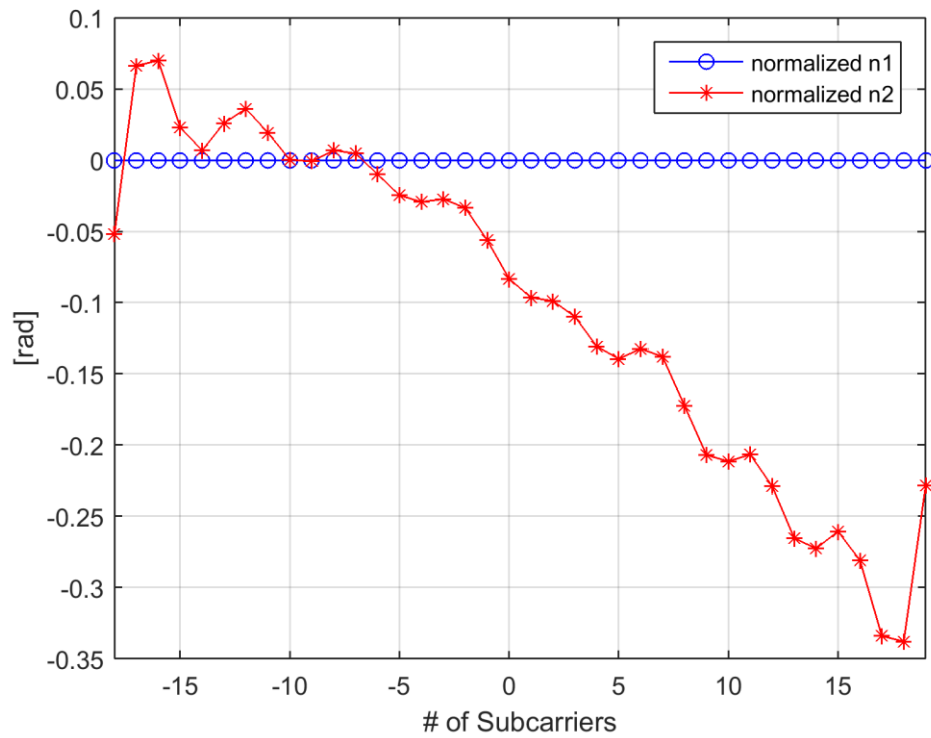
Figure 3.13. *Extracted parameters ($\hat{n}_1$ and $\hat{n}_2$) at BS (phase response)*

Similarly, the normalized FR mismatch parameters at users are calculated as under:

$$\hat{m}_1 = \frac{1}{\sqrt{1+|m_2/m_1|^2}} \tag{30}$$

$$\hat{m}_2 = \frac{e^{j(\varphi_{m2}-\varphi_{m1})}}{\sqrt{1+|m_1/m_2|^2}} \tag{31}$$

The time, frequency and phase responses of normalized frequency mismatch parameters at UE over subcarriers are shown in Figure 3.14, Figure 3.15 and Figure 3.16 respectively.
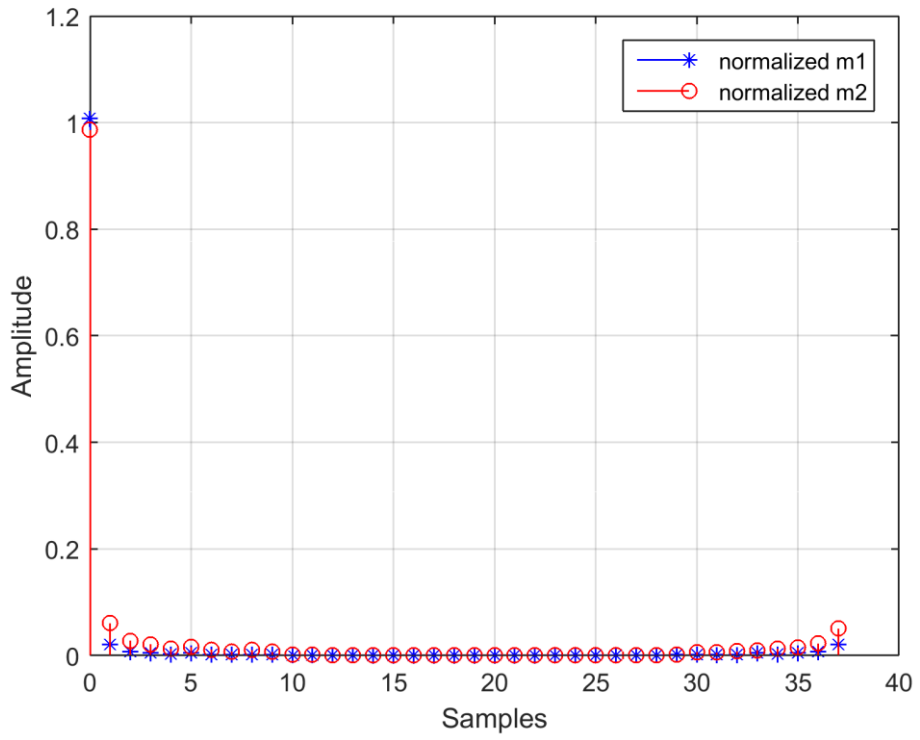
Figure 3.14. *Extracted parameters ($\hat{m}_1$ and $\hat{m}_2$) at UE (time response)*
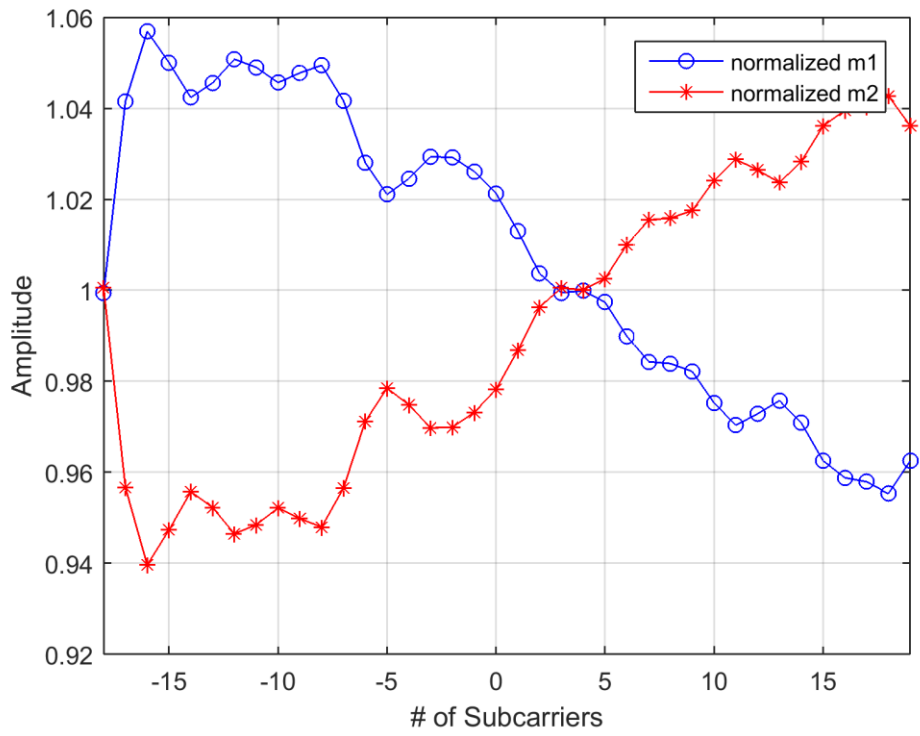
Figure 3.15. *Extracted parameters ($\hat{m}_1$ and $\hat{m}_2$) at UE (frequency response)*
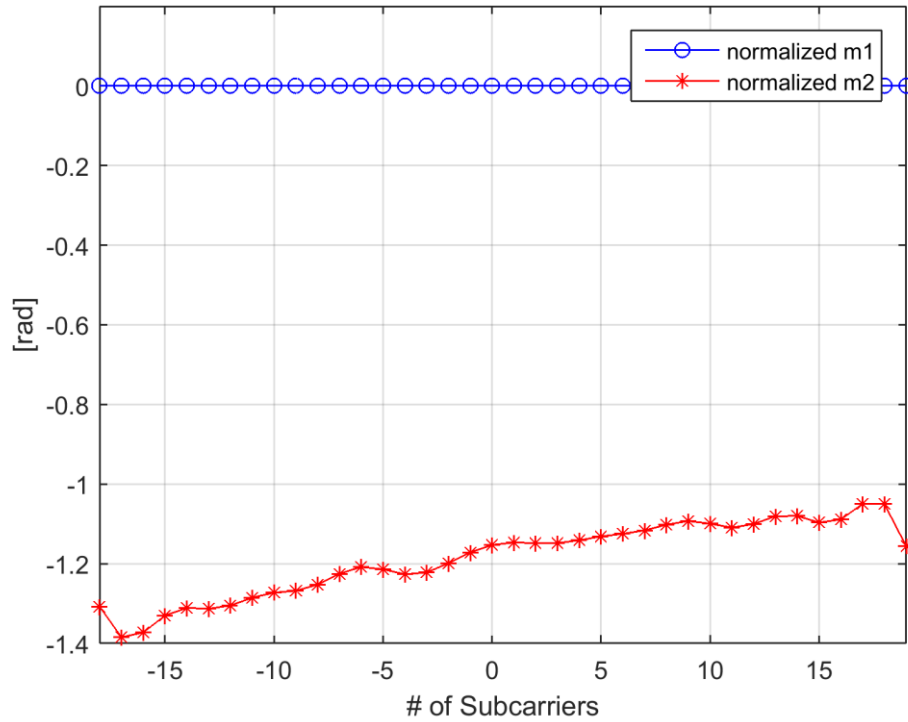
Figure 3.16. *Extracted parameters ($\hat{m}_1$ and $\hat{m}_2$) at UE (phase response)*

Variance is calculated according to the following formulas for BS and UE non-reciprocity coefficients.

$$\sigma_{BS}^2 = \left| \hat{n}_1 - \frac{\hat{n}_1 + \hat{n}_2}{2} \right|^2 + \left| \hat{n}_2 - \frac{\hat{n}_1 + \hat{n}_2}{2} \right|^2 \qquad (32)$$

$$\sigma_{UE}^2 = \left| \hat{m}_1 - \frac{\hat{m}_1 + \hat{m}_2}{2} \right|^2 + \left| \hat{m}_2 - \frac{\hat{m}_1 + \hat{m}_2}{2} \right|^2 \qquad (33)$$

Figure 3.17 illustrates the variance of non-reciprocity at BS and UE (subcarrier-wise). The average variances of transceiver non-reciprocity at BS and UE over subcarriers are -16dB and -5 dB respectively.
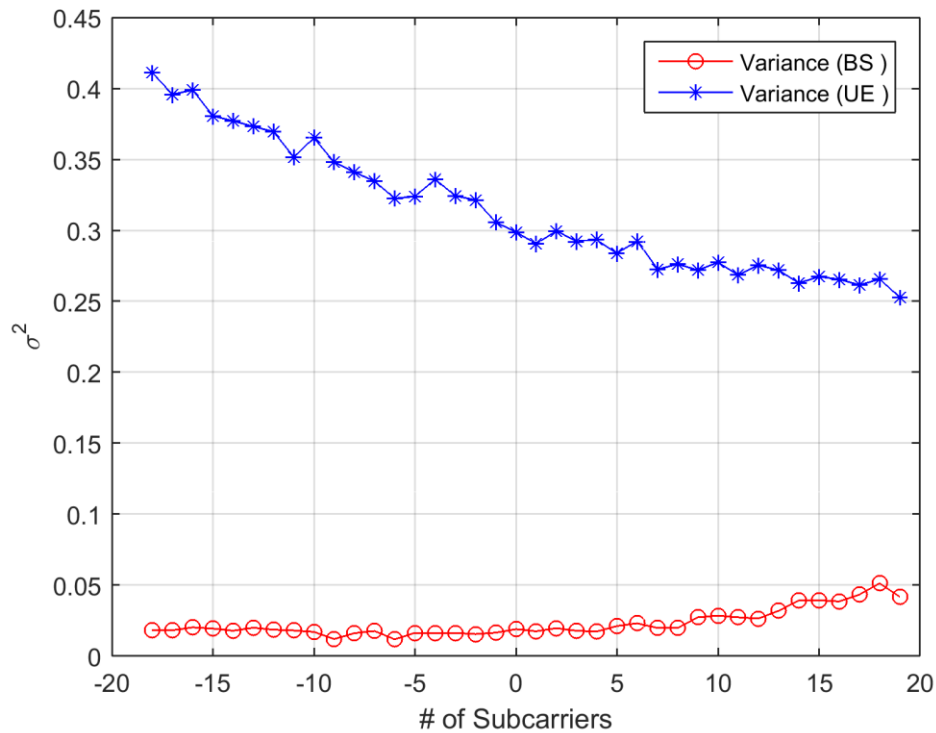
Figure 3.17. *Variance of extracted transceiver non-reciprocity at BS and UE*

From normalized coefficients, following BS and MS FR mismatch coefficients are extracted from measurement data and are used to estimate and compensate the non-reciprocity.

$$\mathbf{A}_b = \begin{bmatrix} \hat{n}_1 & 0 \\ 0 & \hat{n}_2 \end{bmatrix} \tag{34}$$

$$\mathbf{A}_u = \begin{bmatrix} \hat{m}_1 & 0 \\ 0 & \hat{m}_2 \end{bmatrix} \tag{35}$$

3.2 Observations from measurement data results

Each diagonal element of the reciprocity matrix is mildly frequency-selective in frequency-domain. Frequency-selectivity implies reciprocity estimation and compensations are needed subcarrier-wise. Frequency-independent reciprocity estimation and compensation are not sufficient in real world system. The frequency-domain reciprocity are modeled as a FIR filter in the time-domain and the most energy concentrates then on few time-domain taps. Thus, in the presence of additive noise, the quality of frequency-domain reciprocity parameter estimation can be enhanced by nulling most taps to zero. Pilot-based estimation is not needed in every active subcarrier. Sparsely

located pilots structure can be deployed with the use of proper interpolator for lower system overhead.

4. IMPACT OF TRANSCEIVER NON-RECIPROCITY ON THE TDD MU MIMO-OFDM SYSTEM

The chapter presents the impact of FR mismatches on TDD precoded MU MIMO-OFDM system that has been extracted from measurement data. The simulation results are also illustrated for non-reciprocity.

4.1 Analysis of transceiver non-reciprocity

The implementation of MU MIMO-OFDM system is based on two data stream inputs with random bits for each transmit antenna. The block diagram of the simulator that is implemented to analyze non-reciprocity impact is presented in Figure 4.1.

During transmission over the channel, data is distorted due to noisy effects of the channel. As a result, BER is increased. So, error correcting algorithms are used to diminish such type of errors in data transmission over unreliable or noisy communication channels. Error correcting algorithm is basically used to enhance the consistency of the communication by adding some redundancy to the transmitted data bits. Two types of channel coding schemes for error correcting are used such as linear block coding and convolutional coding. The convolutional coding, as an error correcting scheme, is used to encode the channel [38]. In convolutional coding, both data inputs are mapped to the coded bits by taking convolution of data bits with generator sequences. The specifications used for coding algorithm are presented in Table 4-1.

Table 4-1. *Channel coding specifications*

Coefficient Ratios	Value
Rate	1/2
Constraint Length	3
Generator Polynomial	$[7,5]_8$

For mapping the channel coded data streams, 16-QAM digital modulation is used as a subcarrier data modulation. Digital modulation provides more capacity, capability, security, quality and quick availability as compared to analog modulations [14]. There are three constrains (i.e.; bandwidth, power and noise level) of the system while developing any communication system. 16-QAM can encode 4 bits of data in one symbol. Because of high order modulation, it offers faster data rates and higher level of spectral efficiency for the radio communication systems. The higher order modulation schemes are substantially less resistant to interference and noise.
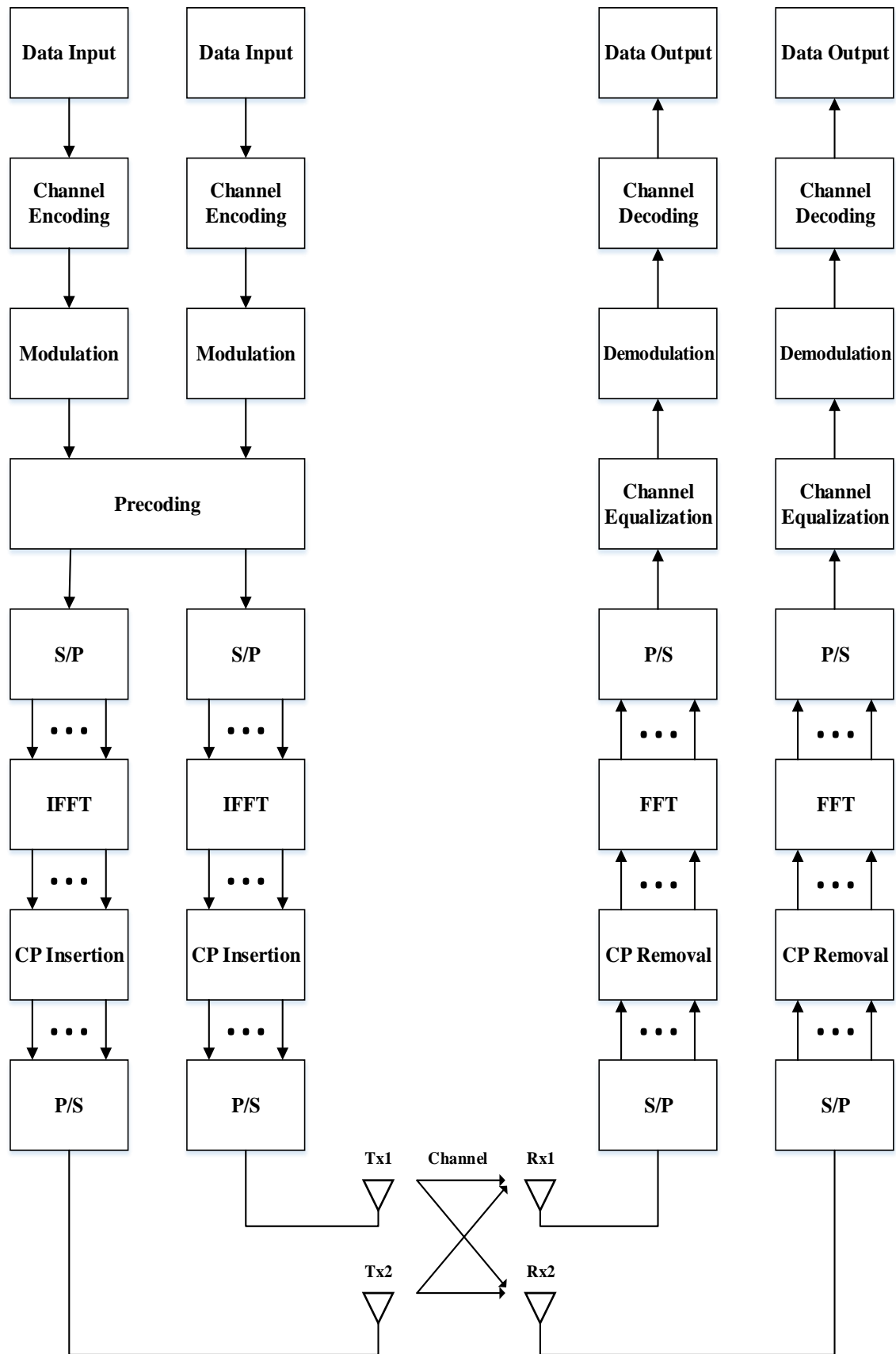
Figure 4.1. *Block diagram for TDD precoded MU MIMO-OFDM system*

After modulation, the pilot sequences are inserted at selected subcarriers of OFDM symbols. It helps to estimate channel efficiently. There are two kinds of technique for inserting pilots [21], [22], [23] at the data subcarriers such as block-type pilot insertion and comb-type pilot insertion. But the sparsely located pilots at selected subcarriers are used in this thesis as shown in Figure 4.2. The base reference sequences (Zhaddoff-Chu) for pilots are generated according to the LTE 3GPP specifications. The sequences have following properties:-

- Flat frequency response
- Circular cross-correlation between two sequences is low with constant magnitude
- Constant amplitude
- Zero circular convolution
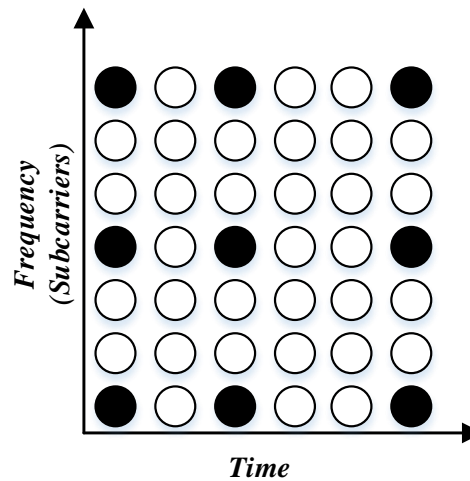
Figure 4.2. *Insertion of pilot sequence*

The data is precoded according to Section 2.4.1. The DL channel is modeled as a Rayleigh fading multipath channel with a given 7-tap channel power delay profile [12], [13], [47]. Figure 4.3 shows the 7-tap channel power delay profile that is used in this thesis for DL channel.

Table 4-2 presents the power specifications in order to compute power delay profile for the DL channels.

Table 4-2. *Parameters for channel power delay profile*

Tap	Power in dB
1	0
2	-1
3	-2
4	-8

7	-17.2
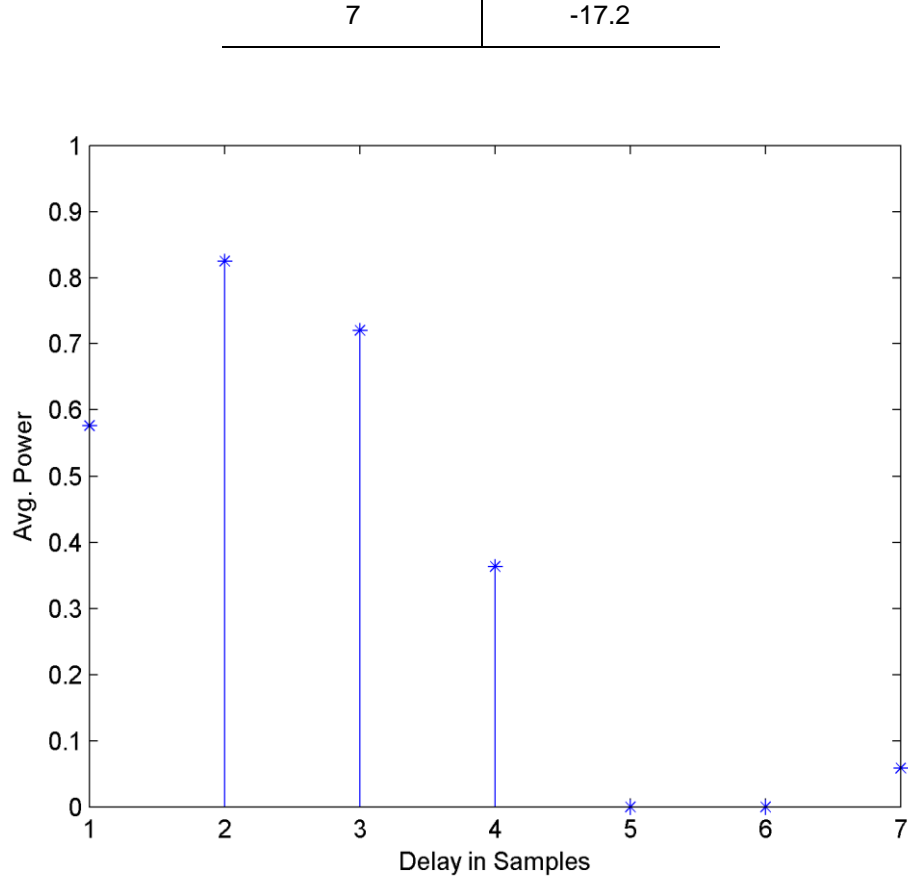
Figure 4.3. *Power delay profile for downlink channel*

When ZF precoding is deployed together with channel non-reciprocity, then $\mathbf{H}_{DL}$ replaces with $\hat{\mathbf{H}}_{DL}$ in equation (11).

$$\hat{\mathbf{H}}_{DL} = \mathbf{A}_b \mathbf{H}_{DL} \mathbf{A}_u \tag{36}$$

$$\mathbf{W}_T = \hat{\mathbf{H}}_{DL}^T (\hat{\mathbf{H}}_{DL} \hat{\mathbf{H}}_{DL}^T)^{-1} \tag{37}$$

Where $\mathbf{A}_b$ is non-reciprocity matrix at BS and $\mathbf{A}_u$ non-reciprocity matrix at UE as calculated in the previous chapter. $\mathbf{W}_T$ is realizable precoder that is calculated by estimating the DL channel in the presence of channel non-reciprocity.

After precoding, the precoded data subcarriers are passed through the channel. The input of the receiver is then corrupted by the addition of noise. Noise is determined by SNR as illustrated below:

$$SNR = 10\log_{10} \frac{P_s}{P_n} \tag{38}$$

Where P_s signal is power and P_n is noise power. It can be rewritten in terms of variances as given below:

$$SNR = 10\log_{10}\frac{\sigma_s^2}{\sigma_n^2} \tag{39}$$

Re-arranging above formula, noise standard deviation can be written as:

$$\sigma_n = \sqrt{\frac{\sigma_s^2}{10^{SNR/10}}} \tag{40}$$

$$\sigma_n = 10^{-SNR/20}\sqrt{\sigma_s^2} \tag{41}$$

To recover data at the receiver, first removal of CP is performed on both transmitted data. FFT is calculated according to OFDM demodulation. After converting into frequency-domain, symbols according to subcarriers are extracted. Channel equalization is done for individual data streams according to the estimated channel. Bits are detected from symbols through demodulation. After demodulation, the channel is decoded to translate detected bits from the code words of a given coding scheme. Viterbi decoder is used for channel decoding. BER is calculated by comparing input bits and decoded bits for both data streams.

The measure of end-to-end performance is done through BER which tells reliability of any system from "bit-in" to "bit-out". When there is no channel non-reciprocity, then BER performance follows the ideal characteristics of TDD precoded MU MIMO-OFDM. But in case of channel non-reciprocity, the performance degrades and does not follow the ideal characteristics.

4.2 Simulated results in case of non-reciprocity

Figure 4.4 and Figure 4.5 illustrate the comparison between uncoded and coded channels respectively in terms of ideal case and when channel non-reciprocity occurs. BER shows the average error rate by comparing both data streams for input and output.

The results illustrate that BER reaches to 10^{-4} at 11dB in case of channel coding and BER cannot reach the 10^{-4} value in case of uncoded channel.
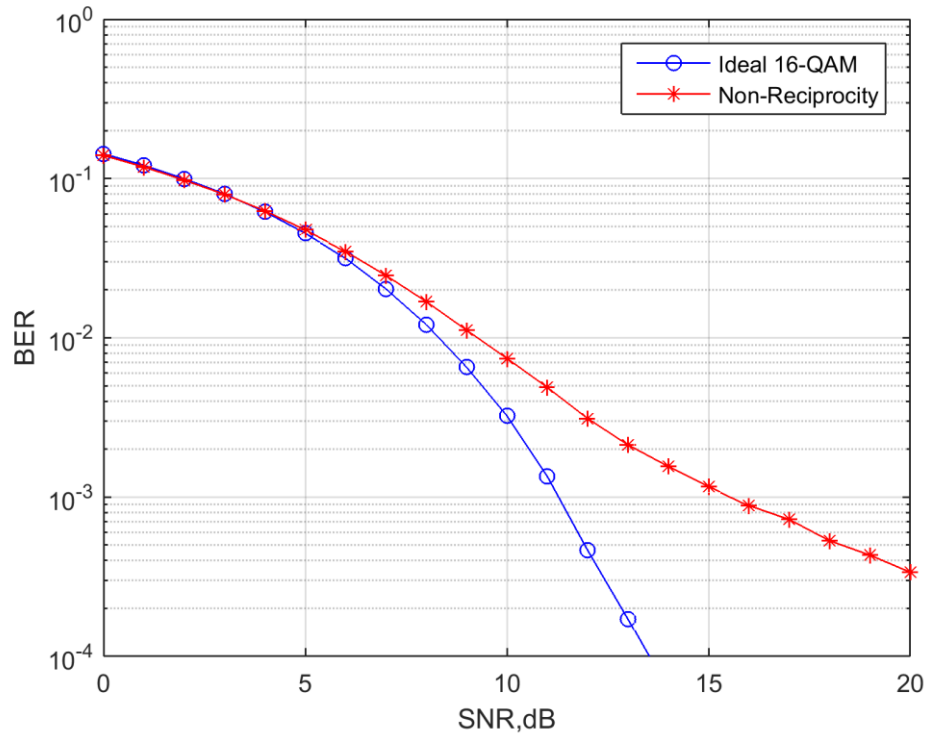
Figure 4.4. *Performance of uncoded channel in presence of non-reciprocity*
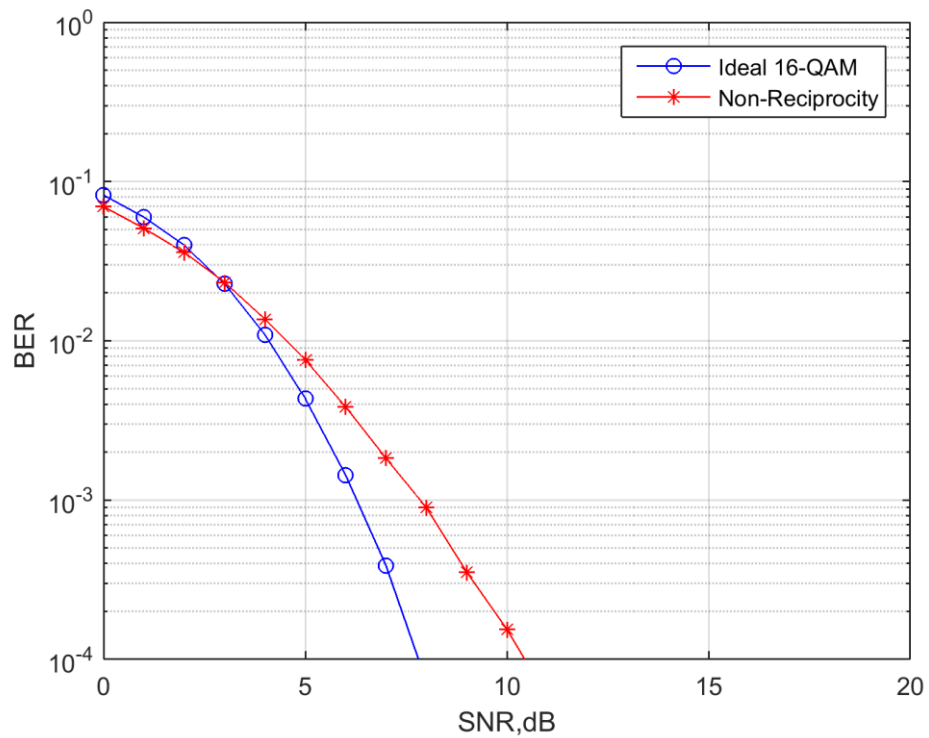
Figure 4.5. *Performance of coded channel in presence of non-reciprocity*

4.3 Summary

The impact of transceiver non-reciprocity is analyzed by implementing simulator of TDD precoded MU MIMO-OFDM system. In this chapter, an effort has been made to implement TDD precoded MU-MIMO OFDM system, It makes use of error correcting algorithm, utilizes 16-QAM digital modulation scheme for high data rates and multicarrier communication technique OFDM for supporting high speed data transmission, employs pilot sequence insertion at selected data subcarriers, provides ZF precoding in order to cancel interference in multi-user communication and offers receiver processing for data detection after adding channel. The impact of non-reciprocity on system performance is less severe when channel coding is deployed as compared to the uncoded data. The next chapter explains the recovery method that compensates the system performance while dealing with non-reciprocity.

5. COMPENSATION OF NON-RECIPROCITY ON THE TDD MU MIMO-OFDM SYSTEM

The efficient algorithm for identification of non-reciprocity is required to solve the non-reciprocity problem. Therefore, estimation of non-reciprocity parameters at BS is carried out to restore the channel reciprocity. In this chapter, the estimation and compensation method for transceiver non-reciprocity (extracted from measurement data) in MU MIMO-OFDM system is explained with the help of work of other researchers [37]. The obtained simulated results are also presented in case of compensated non-reciprocity.

5.1 Estimation of transceiver non-reciprocity

For compensation of transceiver non-reciprocity, there is a need to estimate non-reciprocity parameters at BS transceiver by assuming a link between BS and one of UE devices. The effective UL channel can be written in terms of DL channel and non-reciprocity parameters as:

$$\mathbf{H}_{UL} = \mathbf{A}_b \mathbf{H}_{DL}^T a_e \tag{42}$$

Where a_e is frequency mismatch coefficient for MS1 at UE side (i.e.; m_1). The user selection has prominent impact on estimation of non-reciprocity parameters. The user is selected that has good channel connection in terms of path loss and delay spread with BS. The right choice is helps in noise reduction in estimation. The DL data over subcarriers with sparsely located pilot sequence is denoted as $\mathbf{S}_P^{DL}$. The data is transmitted from BS to UE without ZF precoding. The received signal at UE is given as:

$$\mathbf{R}_P^{DL} = \mathbf{H}_{DL} \mathbf{S}_P^{DL} \tag{43}$$

After computing received signal, the effective DL channel is estimated by deploying pure ZF type inverse processing at UE. The estimated DL channel is calculated as under:

$$\hat{\mathbf{H}}_{DL} = \mathbf{R}_P^{DL} (\mathbf{S}_P^{DL})^{-1} \tag{44}$$

This provides estimates only at the pilot subcarriers. Therefore, linear interpolation is used to obtain channel response estimates at the actual data subcarriers. In contrast to feedback signaling [33], the ZF precoded UL data with pilot sequence is transmitted to BS from UE. The UL data with pilot sequence is denoted as $\mathbf{S}_P^{UL}$ over subcarriers. The transmitted signal from UE to BS is shown below:

$$\mathbf{X}_P^{UL} = \mathbf{S}_P^{UL}(\hat{\mathbf{H}}_{DL})^{-1} \qquad (45)$$

It is assumed that estimated DL channel is perfect for all transmitting antennas. The received signal at BS from UE is given as:

$$\mathbf{R}_P^{UL} = \mathbf{H}_{UL}(\mathbf{X}_P^{UL})^T \qquad (46)$$

$\mathbf{H}_{UL}$ is given in equation (42). The diagonal entries of $\mathbf{R}_P^{UL}$ matrix depend only on the non-reciprocity characteristics. After applying a ZF processing on those diagonal entries of the BS observation matrix with the known pilot sequence $\mathbf{S}_P^{UL}$, an estimate of the non-reciprocity matrix at the BS can be computed:

$$\hat{\mathbf{A}}_b = diag(\mathbf{R}_P^{UL})(\mathbf{S}_P^{UL})^{-1} \qquad (47)$$

$\hat{\mathbf{A}}_b$ is estimated non-reciprocity matrix at BS. The estimated parameters contain data only at pilot position subcarriers. Therefore, linear interpolator is used to obtain estimate for all subcarriers. After interpolation, the resultant parameters are used as a pre-compensator to compensate the non-reciprocity in the system. The mean square error (MSE) is also calculated as shown below by comparing the estimated parameters with the known non-reciprocity characteristics from measurement data:

$$e = \hat{\mathbf{A}}_b - a_e \mathbf{A}_b \qquad (48)$$

$$MSE_{dB} = 10\log_{10}(\sigma_e^2) \qquad (49)$$

The error variance shows the estimation performance that is in the range of -20 dB to -30 dB when 20 dB to 25 dB SNR is used for the additive channel noise in the test link [33].

5.2 Compensation of non-reciprocity

The evaluated non-reciprocity parameters after estimation are used as compensator filter that is applied after data precoding at the BS side. Figure 5.1 shows block diagram for compensated non-reciprocity of precoded MU MIMO-OFDM system. The transmission channel in case of compensator is:

$$\mathbf{H}_T = \mathbf{H}_{DL}\mathbf{W}_C\mathbf{W}_T \qquad (50)$$

$\mathbf{W}_T$ is precoded matrix that is given in equation (37) and $\mathbf{W}_C$ is compensator filter based on estimated non-reciprocity parameters. The remaining steps of the

implementation for detection processing are same as explained in Section 4.1. In this way, optimal solution is used for estimating transceiver non-reciprocity and achieving better performance which is close to the ideal case.
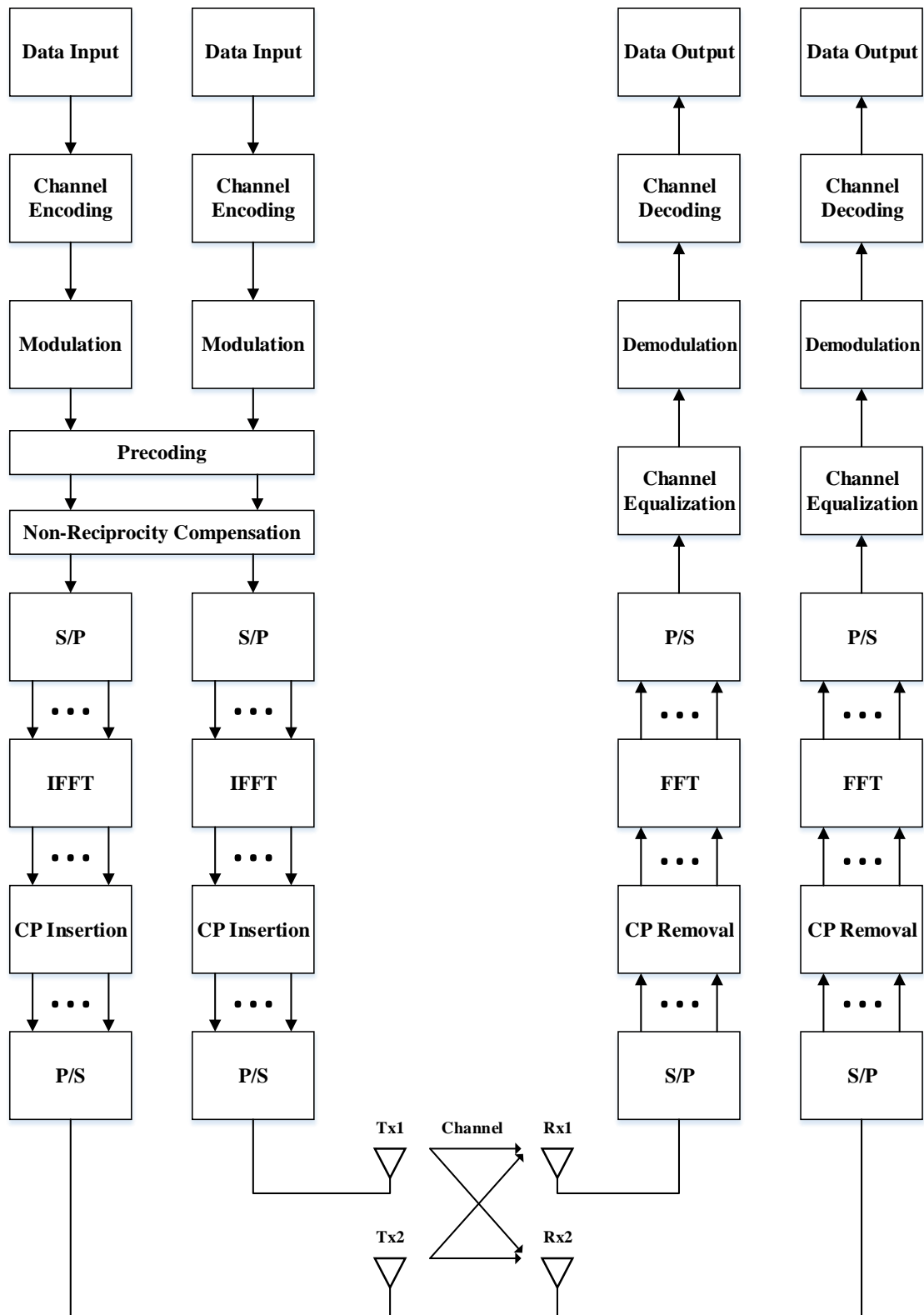
Figure 5.1. *Block diagram for compensated non-reciprocity in TDD precoded MU MIMO-OFDM system*

5.3 Simulated results in case of compensated non-reciprocity

Figure 5.2 describes the performance of estimation through error variance for estimated non-reciprocity parameters in terms of with nulling and without using nulling techniques.
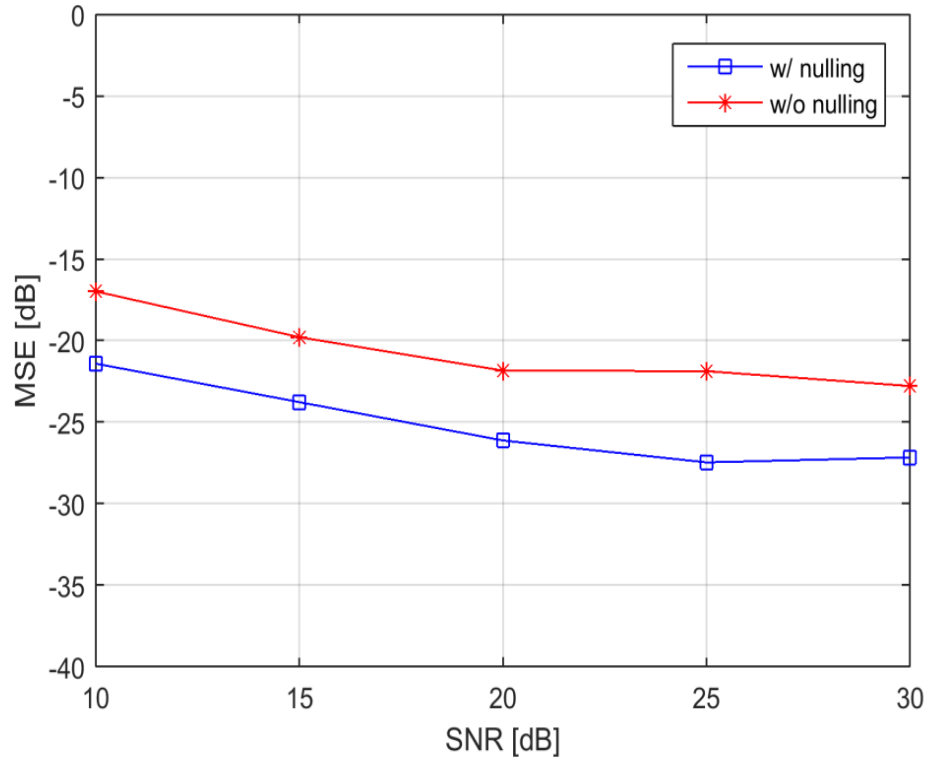
Figure 5.2. *MSE of parameter estimation*

Figure 5.3 and Figure 5.4 present the performance of the system after applying compensator filter in terms of uncoded and coded channel respectively. The compensation performance describes that BER reaches to 10^{-4} at 15 dB in case of uncoded data and 8 dB in case of channel coding. BER shows the average error rate by comparing both data streams at input and output.

Figure 5.3. *Performance of uncoded channel using non-reciprocity compensator*
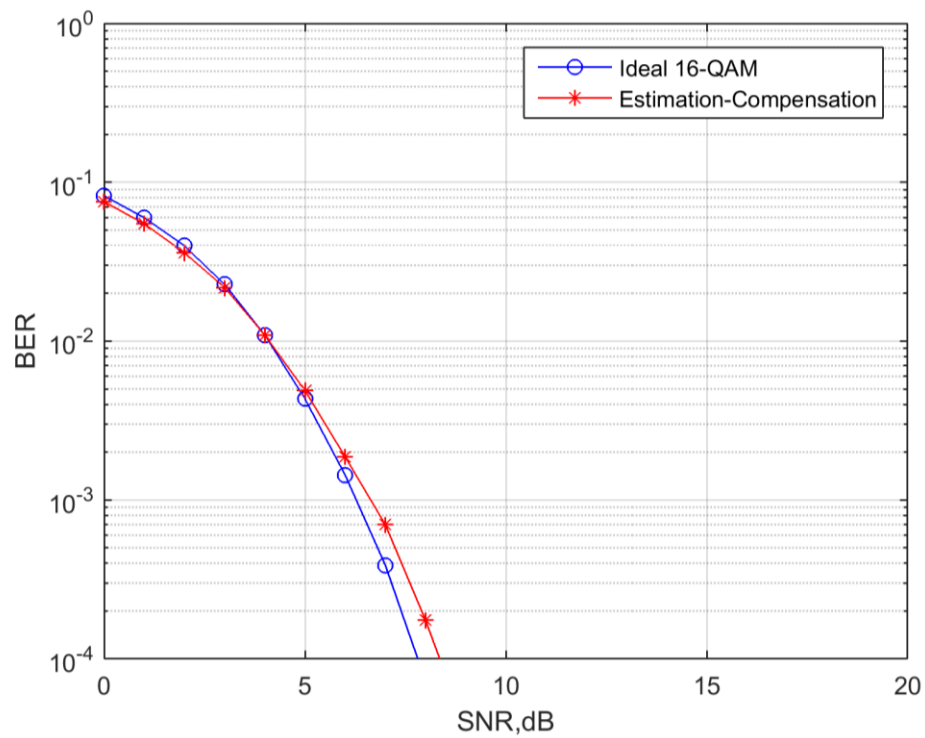
Figure 5.4. *Performance of coded channel using non-reciprocity compensator*

5.4 Summary

In this chapter, the sparsely located pilot-based estimation of non-reciprocity parameters at base-station is carried out in order to compensate the system performance. To estimate channel non-reciprocity parameters, a link between BS and MS1 is taken into account. The DL data including sparsely located pilots at selected subcarriers is transmitted to the user through DL channel. The DL channel is estimated at UE side by using inverse process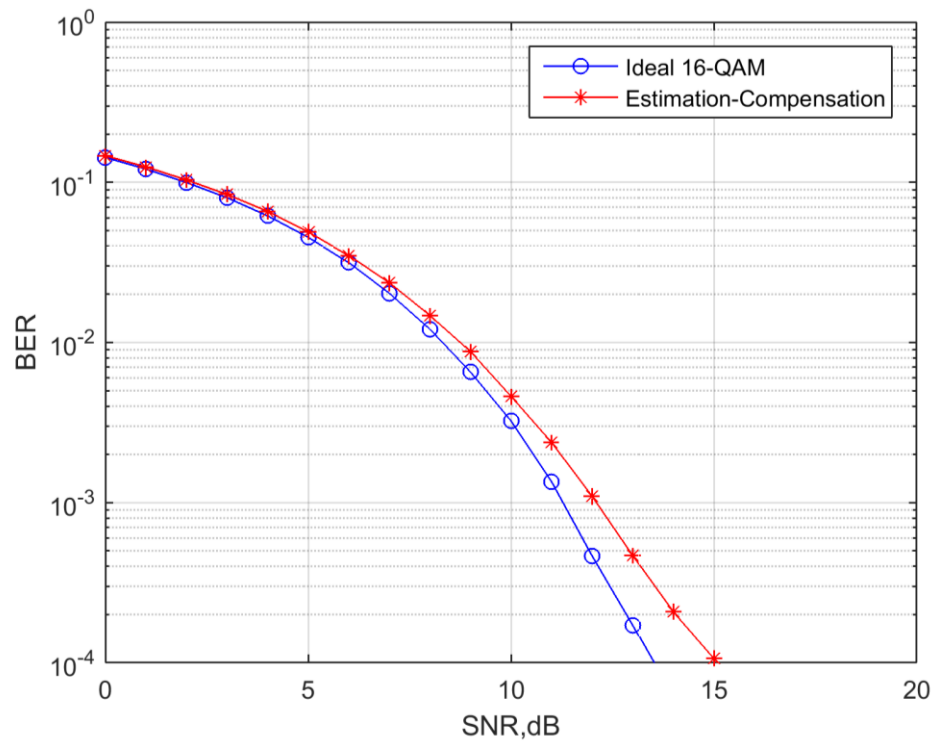ing and an interpolator. The UL pilot data is transmitted to BS from UE side through UL channel. The UL channel is obtained by estimated DL channel in case of non-reciprocity parameters. Then, estimate of non-reciprocity at BS is computed. The estimated parameters are used as a compensator filter to compensate the non-reciprocity in the system. The compensated performance in terms of coded and uncoded channel schemes is evaluated that is close to ideal precoded MU-MIMO OFDM system. The comparison shows that coded channel needs 7 dB less SNR than uncoded channel to achieve 10^{-4} BER.

6. CONCLUSION AND FUTURE WORK

In this chapter, the major contributions of the work are briefly described and possible future work is also given to further enhance the effectiveness of the proposed system.

6.1 Conclusion

There is a need to design FR mismatches at multi-antenna BS by using measurement data in order to ensure the validation of estimation and compensation framework [37] for transceiver non-reciprocity by considering channel reciprocity principle in TDD precoded MU MIMO-OFDM systems. In existing literature, different types of estimation and compensation approaches were studied [32], [33], [34], [35]. But, these approaches cannot be often used because of implementation complexity, high cost equipment, intensive decomposition for channel matrices and limited rate of feedback system from UE to BS. In this research work, non-reciprocity at BS and UE is extracted from actual measurement data and then compensation of extracted non-reciprocity is carried out by estimating non-reciprocity parameters at BS. The proposed approach does not need any use of feedback system and intensive decomposition techniques for channelization.

An effort has been made to extract non-reciprocity matrices at BS and UE which utilize mathematical calculations to implement simulator in order to analyze impact of extracted non-reciprocity in TDD linear precoded MU-MIMO OFDM system. It makes use of error correcting algorithm, modulation schemes and ZF precoding technique to implement simulator in order to compensate the non-reciprocity. The simulator accounts pilot-based estimation process for BS non-reciprocity parameters.

First stage of the implementation shows that all inter-user interference is removed by calibrating reciprocity principle at BS. By using precoding techniques and applying proper detection processing, the impact of transceiver non-reciprocity can be compensated at UE. During the second stage, the realistic FR mismatches from measurement data is added in the implementation to check non-reciprocity effect on the system performance. It causes degradation in performance of MU MIMO-OFDM systems as shown in Figure 4.4 and Figure 4.5 in terms of uncoded and coded channel respectively. To ensure the system reliability and high performance in case of transceiver non-reciprocity, a pilot-based approach for estimating the transceiver non-reciprocity parameters at BS is utilized in the third stage. The estimation provides precise and flexible parameter identification with low computational complexity and system overhead. The estimation error variance with respect to SNR is presented in Figure 5.2.

Using estimated parameter as a compensator, the implemented system can give performance which is close to ideal TDD precoded MU-MIMO OFDM system. The

compensated performance for ZF precoding is presented in Figure 5.3 and Figure 5.4 in terms of uncoded and coded channel respectively. The simulated results describe that the impact of non-reciprocity on system performance is less severe when a coded channel is deployed as compared to the case of uncoded channel. The modeling of transceiver FR mismatch characteristics using realistic measurement data proves that the interference due to transceiver non-reciprocity can be detached with system resources as described in previous research and also verifies that the used model in previous research is close to actuality.

6.2 Future work

Although the proposed system has demonstrated efficient performance to meet the objectives of given research work, but the following future work is suggested for carrying out further analysis and obtaining more results by making use of other schemes.

The implemented approach can be extended to analyze and compensate the non-reciprocity impact in Massive MIMO systems. Integration of I/Q imbalances, PA non-linearity and PLL phase noise in the Massive MIMO systems can be considered for further analysis in case of non-reciprocity:

DL and UL transmission using multi-cells can be considered for detailed performance analysis. The actual system can be implemented in order to obtain more accurate and precise estimation results.

REFERENCES

[1]   3GPP Technical Specification Group Radio Access Network, "High speed downlink packet access (HSDPA); Overall description; Stage 2," technical specification TS 25.308, Version 8.1.0, 2008.

[2]   3GPP Technical Specification Group Radio Access Network, "User equipment (UE) radio transmission and reception (FDD)," technical specification TS 25.101, Version 8.2.0, 2008.

[3]   3GPP Technical Specification Group Radio Access Network, "LTE physical layer- General description," TR 36.201, 2007.

[4]   3GPP Technical Specification Group Radio Access Network, "Overall description of E-UTRA/E-UTRAN; Stage 2," TR 36.300, Version 8.3.0, 2007.

[5]   J.H. Winters, "On the capacity of radio communication systems with diversity in a Rayleigh fading environment," IEEE Journal on Selected Areas in Communications, Volume 5, Number 5, pp. 871-878, 1987.

[6]   I. E. Telatar, "Capacity of multi-antenna Gaussian channels," European Transactions on Telecommunications, Volume 10, Number 6, pp. 585–595, 1995.

[7]   T. L. Marzetta and B. M. Hochwald, "Capacity of a mobile multiple-antenna communication link in Rayleigh flat fading," IEEE Transactions on Information Theory, Volume 45, Number 1, pp. 139–157, 1999.

[8]   P. Frank, A. Müller, and J. Speidel, "Performance of CSI-based multi-user MIMO for the LTE downlink," Proceedings of 6th International Wireless Communications and Mobile Computing Conference (IWCMC), USA, pp. 1086–1090, 2010.

[9]   P. Frank, A. Müller, H. Droste, and J. Speidel, "Cooperative interference-aware joint scheduling for the 3GPP LTE uplink," Proceedings of IEEE 21st International Symposium on Personal Indoor and Mobile Radio Communications (PIMRC), pp. 2216–2221, 2010.

[10]   A. Soysal and S. Ulukus, "Optimum power Allocation for Single-User   MIMO and Multi-User MIMO-MAC with Partial CSI," IEEE Transactions on Selected Areas in Communications, Volume. 25, Number 7, pp. 1402–1412, 2007.

[11]   S. Serbetli and A. Yener, "Transceiver Optimization for Multiuser MIMO Systems," IEEE Transactions on Signal Processing, Volume. 52, Number 1, pp. 214–226, 2004.

[12]   T. B. Sorensen, P. E. Mogensen, and F. Frederiksen, "Extension of the ITU channel models for wideband (OFDM) systems," IEEE Vehicular Technology, Conference (VTC2005-Fall), pp. 392-396, September 2005.

[13]   H. Holma and A. Toskala, "LTE for UMTS: Evolution to LTE-Advanced," Second Edition, West Sussex, 2011.

[14]   Hewlett-Packard, "Digital Modulation in Communications Systems – An Introduction," Application Note 1298, 1997. [Accessed 13.08.2015]. Available: http://cp.literature.agilent.com/litweb/pdf/5965-7160E.pdf

[15]   Q. H. Spencer, A. L. Swindlehurst, and M. Haardt, "Zero-forcing methods for downlink spatial multiplexing in multiuser MIMO channels," IEEE Transactions on Signal Processing, Volume 52, Number 2, pp. 461–471, 2004.

[16]   A. Wiesel, Y. C. Eldar, and S. Shamai, "Zero-Forcing Precoding and Generalized Inverses," IEEE Transactions on Signal Processing, Volume 56, Number 9, September 2008.

[17]   Y. G. Li, L.J. Cimini and N. R. Sollenberger, "Robust channel estimation for OFDM system with rapid diverse fading channels," IEEE Transaction on Communication, Volume 46, Number 7, pp. 902-914, July 1998.

[18]   O. Edfors, M. Sandell, J.-J. Van de Beek, D. Landström, and F. Sjöberg, "An Introduction to Orthogonal Frequency Division Multiplexing," Sweden: Luleå Tekniska Universitet, pp. 1–58, 1996.

[19]   M. Hsieh and C. Wei, "Channel Estimation for OFDM Systems Based on Comb-type Pilot Arrangement in Frequency Selective Fading Channels," IEEE Transactions on Consumer Electronics, Volume 44, Number 1, pp. 217-225, 1998.

[20]   Y. Li, "Pilot-Symbol-Aided Channel Estimation for OFDM in Wireless Systems," IEEE Transactions on Vehicular Technology, Volume 49, Number 4, pp 1207-1215, 2000.

[21]   S. Yushi and M. Ed, "Channel Estimation in OFDM Systems," Freescale Semiconductor Application Note, 2006. [Accessed 12.08.2015]. Available: http://www.freescale.com/files/dsp/doc/app_note/AN3059.pdf

[22] G. Fodor, P. Di Marco, and M. Telek, "Performance analysis of block and comb type channel estimation for massive MIMO systems," IEEE Transactions on 5G for Ubiquitous Connectivity, pp. 62-69, November 2014.

[23] R. H. Khimani, J. K. Bhalani, and J. M. Rathod, "Comparison and Performances of Pilot Based Channel Estimation Techniques for MIMO–OFDM System with Different Modulation Schemes," Volume 2, April 2013.

[24] G. Tsoulos, "MIMO System Technology for Wireless Communications," New York: CRC Press, 2006. [Accessed 12.08.2015]. Available: https://www.crcpress.com/MIMO-System-Technology-for-Wireless-Communications/Tsoulos/9780849341908

[25] B. Z. Maha, and K. Kosai, "Multi User MIMO Communication: Basic Aspects, Benefits and Challenges," Paper distributed under the terms of the Creative Commons Attribution License, 2013. [Accessed 12.08.2015]. Available: http://cdn.intechopen.com/pdfs-wm/45873.pdf

[26] M. Codreanu, A. Tolli, M. Juntti, and M. Latva-aho, "Joint Design of Tx-Rx Beamformers in MIMO Downlink Channel," IEEE Transactions on Signal Processing, Volume 55, Number 9, pp. 4639–4655, 2007.

[27] K. Gomadam, V. R. Cadambe, and S. A. Jafar, "A Distributed Numerical Approach to Interference Alignment and Applications to Wireless Interference Networks," IEEE Transactions on Information Theory, Volume 57, Number 6, pp. 3309–3322, 2011.

[28] A. Tarighat, M. Sadek, and A. H. Sayed, "A multi user beamforming scheme for downlink MIMO channels based on maximizing signal-to-leakage ratios," IEEE International Conference on Acoustics, Speech, and Signal Processing (ICASSP), Volume 3, pp. iii/1129–iii/1132, 2005.

[29] Lu. Lu, Ye. Li. Georgia, A. Lee, A. Alexei, and Z. Rui, "An Overview of Massive MIMO: Benefits and Challenges," IEEE Journal of Selected Topics in Signal Processing, Volume 8, pp. 742-758, 2014.

[30] T. L, Marzetta, "How much training is required for multiuser MIMO?," 40th Asilomar Conf. Signals, Systems and Comput. (ACSSC), pp. 359–363, 2006.

[31] T. L. Marzetta, "Non-cooperative cellular wireless with unlimited numbers of base station antennas," IEEE Transaction on Wireless Communication, Volume 9, Number 11, pp. 3590–3600, 2010.

[32] L. Bruhl, C. Degen, W. Keusgen, B. Rembold, and C. M. Walke, "Investigation of front-end requirements for MIMO-systems using downlink pre-distortion," in

Proc. European Personal Mobile Communication Conference., pp. 472- 476, 2003.

[33]   M. Petermann, M. Stefer, F. Ludwig, D. Wubben, M. Schneider, S. Paul, and K. Kammeyer, "Multi-User Pre-Processing in Multi-Antenna OFDM TDD Systems with Non-Reciprocal Transceivers," IEEE Transactions on Communications, Volume 61, Number 9, pp. 3781-3793, 2013.

[34]   B. Kouassi, I. Ghauri, and L. Deneire, "Estimation of time-domain calibration parameters to restore MIMO-TDD channel reciprocity," Cognitive Radio Oriented Wireless Networks and Communications (CROWNCOM), pp. 254-258, 2012.

[35]   P. Zetterberg, "Experimental Investigation of TDD Reciprocity-Based Zero-Forcing Transmit Precoding," EURASIP Journal on Advances in Signal Processing, Volume 2011, 2011.

[36]   J. Zhang, J. G. Andrews, and R. W. Heath, "Block Diagonalization in the MIMO Broadcast Channel with Delayed CSIT," IEEE Global Telecommunications Conference (GLOBECOM), pp. 1–6, 2009.

[37]   Z. Yaning, O. Raeesi, and M. Valkama, "Efficient estimation and compensation of transciever non-reciprocity in precoded TDD multi-user MIMO-OFDM Systems," Vehicular Technology Conference (VTC Fall), pp. 1-7, 2014.

[38]   L. Hanzo, T. Liew, B. Yeap, and R. Tee, "Convolutional Channel Coding," Wiley-IEEE Press, Edition 1, pp. 13-23, 2011.

[39]   D. Tse and P. Viswananth, "Fundamentals of wireless Communication," Cambridge Univeristy Press, 2005.

[40]   G. J. Foschini, "On limits of wireless communications in a fading environment when using multiple antennas," Wireless Personal Communication, Volume 6, pp. 311-335, 1998.

[41]   B. Widrow, P. E. Mantey, L. J. Griffiths, and B. B. Goode, "Adaptive antenna systems," Proc. IEEE, Volume 55, pp. 2143-2159, 1967.

[42]   S. M. Alamouti, "A simple transmit diversity technique for wireless communications," IEEE J. Sel. Areas Communication, Voulume 16, pp. 1451-1458, 1998.

[43]   A. Paulraj, R. Nabar, and D. Gore, "Introduction to space time wireless communications," Cambridge, UK, 2003.

[44]   A. V. Zelst, "Space division multiplexing algorithms," In Proc. Mediterranean Electrotech. Conference, Volume 3, pp. 1218-1221, 2000.

[45]   T. Parfait, Y. Kuang and K. Jerry, "Performance Analysis and Comparison of ZF and MRT Based Downlink Massive MIMO Systems," Ubiquitous and Future Networks (ICUFN), pp. 383-388, 2014.

[46]   Y. Lim, C. Chae and G. Caire, "Performance Analysis of Massive MIMO for Cell-Boundary Users," IEEE Transactions on Wireless Communications, Volume PP, pp. 1, 2015.

[47]   K. J. R. Liu, A. K. Sadek, S. Weifeng, and A. Kwasinski, "Background and MIMO systems," Cambridge University Press, 2008

[48]   A. Paulraj, and T. Kailath, "Increasing capacity in wireless broadcast systems using distributed transmission/directional reception (DTDR)," US Patent No. 5,345,599, Issued 1993.